EPOXY/TRIAZINE BASED HIGH PERFORMANCE MOLDING COMPOUND FOR NEXT GENERATION POWER ELECTRONICS PACKAGING

A Dissertation
Presented to
The Academic Faculty

by

Jiaxiong Li

In Partial Fulfillment
of the Requirements for the Degree
Master of Science in the
Materials Science and Engineering

Georgia Institute of Technology
[August 2019]

COPYRIGHT © 2019 BY JIAXIONG LI

EPOXY/TRIAZINE BASED HIGH PERFORMANCE MOLDING COMPOUND FOR NEXT GENERATION POWER ELECTRONICS PACKAGING

Approved by:

Dr. C.P. Wong, Advisor
School of Materials Science and Engineering
Georgia Institute of Technology

Dr. Meilin Liu
School of Materials Science and Engineering
Georgia Institute of Technology

Dr. Zhiqun Lin
School of Materials Science and Engineering
Georgia Institute of Technology

Date Approved: [July 12, 2019]

[To my family]

ACKNOWLEDGEMENTS

I would like to express my appreciation to my advisor, Dr. CP Wong for his inspiration and guidance through my graduate study. His focus on details and fundamentals have made great influence on my way of thinking. I also want to thank Dr. Meilin Liu and Dr. Zhiqun Lin for serving as my committee member and for their valuable suggestions.

I want to thank Dr. Kyoung-sik (Jack) Moon for his help and many useful discussions on my research work, without which I could not make such progress in the projects. I would also like to express my gratitude to Dr. Rao Tummala, Dr. Madhavan Swaminathan, Dr. Vanessa Smet and Dr. Kathaperumal (Mohan) Mohanalingam from Packaging Research Center (PRC) for their encouragement and help during my research task. Special thanks to Dr. Lukas Graber from School of Electrical and Computer Engineering and Dr. Shannon Yee from School of Mechanical Engineering for sharing the research equipment. I also want to extent my appreciation to the staff in PRC and School of Materials Science and Engineering (MSE), they are Ms. Dracy Blackwell, Ms. Teresa Nelson, Mr. Chris White, Mr. Lila Dahal, Ms. Chelsea Heath, Mr. Brian McGlade and Ms. Nykia Olds.

I would like to acknowledge all the helps I received from the members in Dr. Wong's group and Dr. Tummala's group. They are Dr. Bo Song, Ms. Fan Wu, Dr. Rong Zhang, Mr. Jinho Hah, Dr. Cheng Zhang, Mr. Zhijian Sun, Mr. Dong An, Mr. Sheng Xu and Mr. Xiaofei Zhang from Dr. Wong's group, and Mr. Haksun Lee, Mr. Bartlet Deprospo, Mr. Nobuo Ogura and Dr. Chandrasekharan Nair from Dr. Tummala's group.

Special thanks to Mr. Chao Ren from our group who has been dedicated to assist me in preparing samples and performing the research.

This work is funded by the Packaging Research Center of Georgia Tech. Special appreciation is extended to the Institute of Electronics and Nanotechnology (IEN) and the Materials Innovation and Learning Laboratory in MSE for the assistance in characterization tools. Thanks to the Lonza compony especially to Ms. Delane Tomlinson for their help and kindly supplying the gratis samples.

TABLE OF CONTENTS

ACKNOWLEDGEMENTS	**IV**
LIST OF TABLES	**VII**
LIST OF FIGURES	**IX**
LIST OF SYMBOLS AND ABBREVIATIONS	**XIII**
SUMMARY	**XV**
CHAPTER 1. Introduction	**1**
1.1 Trends in Power Electronics Packaging	**1**
1.2 Overview of Epoxy Molding Compound	**4**
1.3 Criteria and Approaches on High Temperature Polymeric Material	**7**
1.4 The Development of Cyanate Ester and Epoxy Copolymer System	**10**
1.5 Research Objectives and Outline	**16**
CHAPTER 2. Development and Evaluation on Biphenyl Epoxy/Triazine Based High Temperature Stable Resin Systems	**19**
2.1 Materials and Experimental	**19**
2.2 Metal Catalyst Optimization and Curing Reaction Study in Cyanate Ester/ Epoxy System	**21**
2.3 Direct Insertion of Triazine Functions in Cyanate Ester/ Epoxy system	**31**
2.4 Development of Novolac Type Cyanate Ester/ Epoxy Copolymer System	**40**
2.5 Conclusion	**53**
CHAPTER 3. Development and Failure Analysis of Novolac Epoxy/Triazine Based High Temperature Stable Resin Systems	**56**
3.1 Materials and Experimental	**56**
3.2 Screen Test on Novolac Type Epoxy/Triazine Copolymers	**57**
3.3 Evaluation on Epoxy Cresol Novolac/Triazine Resin System	**61**
3.4 High Temperature Aging Effects on Epoxy Cresol Novolac/Triazine Copolymers	**73**
3.5 Conclusion	**86**
CHAPTER 4. Summary and Suggested Work	**89**
4.1 Summary	**89**
4.2 Suggested Work	**92**
REFERENCES	**94**
PUBLICATIONS OF THE AUTHOR	**101**

LIST OF TABLES

Table 2.2-1 Parameters from TGA thermogram of CE cured with Al(III) acac, Cu(II) acac and Cu(II) bzac in N2, including the temperature at 5% and 10% weight loss and residue weight at 800 ºC. 26

Table 2.2-2 TMA thermomechanical properties of CE cured with Al(III) acac, Cu(II) acac and Cu(II) bzac, including the Tg and CTE before and after glass transition. 27

Table 2.3-1 Parameters from TMA tests on cured CE/EP and TGIC incorporated CE/EP, including the Tg and CTE before and after glass transition. 34

Table 2.3-2 DMA thermomechanical properties of CE/EP and TGIC incorporated CE/EP, including Tg, storage moduli at rubbery region and the calculated crosslink density accordingly. 35

Table 2.3-3 Summarized parameters from TGA thermogram of CE/EP and TGIC incorporated CE/EP in N2 and air atmosphere, including the temperature at 5% and 10% weight loss and residue weight at 800 ºC (in N2). 38

Table 2.3-4 Moisture absorption of CE/EP and the TGIC incorporated CE/EP. Data was selected based on the saturation weight gain in 105 ºC/ 100 RH HAST chamber. 39

Table 2.4-1 Parameters from TMA tests on NCE/ EP blends including the Tg and CTE before and after glass transition. 44

Table 2.4-2 DMA thermomechanical properties of the NCE/ EP blends, including Tg, storage moduli at rubbery region and the calculated crosslink density. 46

Table 2.4-3 Summarized parameters from TGA thermogram of the NCE/ EP blends, including the temperature at 5% and 10% weight loss and residue weight at 800 ºC. 48

Table 2.4-4 Dielectric constant and loss factor of NCE and the NCE/ EP blends at 10 MHz. 50

Table 3.2-1 Comparison of TMA Tg of CE/TMBP blend and CE/ECN blend. (epoxide: cyanate molar ratio at 1:1) 60

Table 3.3-1	Parameters from TMA tests on CE/ECN blends including the Tg and CTE before and after glass transition.	64
Table 3.3-2	DMA thermomechanical properties of the CE/ECN blends, including Tg, storage moduli at rubbery region and the calculated crosslink density.	68
Table 3.3-3	Summarized parameters from TGA and DTG thermogram of the CE/ECN blends, including the temperature at 5% and 10% weight loss, residue weight at 800 ºC, initial decomposition temperature and peak decomposition temperature.	71
Table 3.3-4	Dielectric constant and loss factor of CE/ECN blends at 10 MHz.	72
Table 3.4-1	Parameters from TMA tests on CE/ECN blends during aging under 250 ºC aging including the Tg and CTE before and after glass transition.	76
Table 3.4-2	Summarized parameters from TGA and DTG thermogram of the CE/ECN blends after aging under 250 ºC for different time, including the temperature at 5% and 10% weight loss, residue weight at 800 ºC, initial decomposition temperature and peak decomposition temperature .	84

LIST OF FIGURES

Figure 1.1.1	The structure of a typical power package SO-8 [1].The structure of a typical power package SO-8 [1].	3
Figure 1.2.1	Example of EMC in a package [10].	5
Figure 1.2.2	Comparison of molding method [10].	6
Figure 1.4.1	Reaction mechanism of CE trimerization through phenol impurities [54].	12
Figure 1.4.2	Reaction mechanism of CE trimerization catalyzed by metal ions [54].	12
Figure 1.4.3	Schematic representation of reactions happen in a CE/EP copolymer system.	15
Figure 1.4.4	The reaction route of carbamate formation through the hydrolysis of cyanate groups and its decomposition that lead to out gas.	16
Figure 2.2.1	DSC thermogram of uncatalyzed CE.	22
Figure 2.2.2	Chemical structure of Al(III) acac, Cu(II) acac and Cu(II) bzac.	23
Figure 2.2.3	DSC thermograms of CE catalyzed by Al(III) acac, Cu(II) acac and Cu(II) bzac.	24
Figure 2.2.4	FTIR spectra of CE cured with Al(III) acac, Cu(II) acac and Cu(II) bzac.	25
Figure 2.2.5	TGA thermogram of CE cured with Al(III) acac, Cu(II) acac and Cu(II) bzac, in N_2.	26
Figure 2.2.6	Weight loss profile of CE cured with Al(III) acac, Cu(II) acac and Cu(II) bzac under storage at 200 ºC.	28
Figure 2.2.7	DSC curing thermogram of pure CE/EP blend and its mixture with Al(III) acac, Cu(II) acac and Cu(II) bzac.	29
Figure 2.2.8	FTIR spectra of CE/EP with Cu (II) acac catalyst during temperature ramp.	30
Figure 2.3.1	DSC curing profile of CE/EP and TGIC incorporated CE/EP.	32

Figure 2.3.2	FTIR spectra at 1000 cm^{-1} to 2000 cm^{-1} region of cured CE/EP and TGIC incorporated CE/EP.	33
Figure 2.3.3	DMA tan δ profiles of CE/EP and TGIC incorporated CE/EP.	35
Figure 2.3.4	TGA profile of CE/EP and TGIC incorporated CE/EP in N_2 atmosphere. The inset magnifies the 300-400 ℃ region.	37
Figure 2.3.5	TGA profile of CE/EP and TGIC incorporated CE/EP in air atmosphere.	37
Figure 2.3.6	Weight loss under 250 ℃ aging of CE, CE/EP and the TGIC incorporated CE/EP.	39
Figure 2.3.7	FTIR spectra of CE/EP and the TGIC incorporated CE/EP at 2750 cm^{-1}~ 3750 cm^{-1} region.	40
Figure 2.4.1	Structure of the NCE used in this study.	41
Figure 2.4.2	DSC curing thermogram of the pure NCE and the NCE/ EP blends at different ratio.	42
Figure 2.4.3	Viscosity of the uncured NCE and the NCE/EP blends during temperature ramp.	43
Figure 2.4.4	Chemical structures of NCE and the NCE/ EP blends.	44
Figure 2.4.5	DMA tan δ profiles of NCE and the NCE/ EP blends.	46
Figure 2.4.6	TGA thermogram of NCE and the NCE/ EP blends in N_2.	48
Figure 2.4.7	Moisture absorption of NCE and the NCE/ EP blends under 85 ℃/85 RH condition.	50
Figure 2.4.8	Weight loss under 250 ℃ aging of NCE and the NCE/ EP blends.	52
Figure 2.4.9	Picture of the NCE and the NCE/ EP blends under 250 ℃ aging, the number above the picture denotes the formulation of the copolymers.	52
Figure 3.2.1	Chemical structure of typical epoxy phenol novolac (EPN) and epoxy cresol novolac (ECN).	58
Figure 3.2.2	TGA thermogram of the copolymer between CE and two types of EPN, one ECN and the previously used TMBP. The inset magnifies the 350 ℃~ 425 ℃ region.	59

Figure 3.2.3	Weight loss under 250 ºC aging of the copolymer between CE and two types of EPN, one ECN and the previously used TMBP.	60
Figure 3.3.1	DSC curing thermogram of the CE/ECN blends at different ratio , ranging from 1:3 to 3:1 on molar ratio between cyanate groups and epoxide groups.	62
Figure 3.3.2	FTIR spectra of CE/ECN blends at 1: 1 molar ratio during temperature ramp.	63
Figure 3.3.3	FTIR spectra of CE/ECN blends with different feed ratio.	64
Figure 3.3.4	DMA tan δ profiles of CE/ECN blends ranging from 1:3 to 3:1 on molar ratio.	67
Figure 3.3.5	DMA tan δ profiles of CE/ECN blends ranging from 1:3 to 1:2 on molar ratio.	67
Figure 3.3.6	TGA thermogram of CE/ECN blends in N_2. The inset magnifies the 350 ºC~ 450 ºC region.	70
Figure 3.3.7	DTG thermogram of CE/ECN blends in N_2.	70
Figure 3.3.8	Moisture absorption of CE/ECN blends under 85 ºC/85 RH condition.	72
Figure 3.4.1	Weight loss under 250 ºC aging of CE/ ECN blends.	74
Figure 3.4.2	Pictures of CE/ ECN blends under 250 ºC aging. The number on top of the picture denotes the formulation of the copolymer.	74
Figure 3.4.3	FTIR spectra of CE/ECN 1:3 blend during 250 ºC aging.	79
Figure 3.4.4	FTIR spectra of CE/ECN 1:1 blend during 250 ºC aging.	79
Figure 3.4.5	FTIR spectra of CE/ECN 3:1 blend during 250 ºC aging.	80
Figure 3.4.6	(a) TGA and (b)DTG thermogram of CE/ECN 1:3 blends after aging in 250 ºC for different time in N_2. The inset in (a) magnifies the 350 ºC~ 450 ºC region.	83
Figure 3.4.7	Normalized TGA thermogram of CE/ECN 1:3 blends after aging in 250 ºC for different time in N_2. The inset magnifies the 400 ºC~ 440 ºC region.	83
Figure 3.4.8	(a) TGA and (b)DTG thermogram of CE/ECN 1:1 blends after aging in 250 ºC for different time in N_2.	84

Figure 3.4.9 (a) TGA and (b)DTG thermogram of CE/ECN 3:1 blends after aging in 250 ºC for different time in N_2. 84

LIST OF SYMBOLS AND ABBREVIATIONS

EMC	Epoxy Molding Compound
EP	Epoxy
CE	Cyanate Ester
TGIC	Triglycidyl Isocyanurate
EV	Electric Vehicles
HEV	Hybrid Electric Vehicles
MOSFET	Metal-Oxide Semiconductor Field Effect Transistor
IGBT	Insulated Gate Bipolar Transistor
CTE	Coefficient of Thermal Expansion
IC	Integrated Circuit
SOC	System on Chip
SiP	System in package
WBG	Wide Band Gap
T_g	Glass Transition Temperature
BGA	Ball Grid Array
WL-CSP	Wafer Level- Chip Scale Package
TGA	Thermal Gravimetric Analysis
HDT	Heat Distortion Temperature
EPN	Epoxy Phenol Novolac
ECN	Epoxy Cresol Novolac
PEI	Polyetherimide
PES	Polyethersulfone

PEEI	Poly (Ether Ether Ketone)
BMI	Bismaleimide
BCB	Benzocyclobutene
PCB	Printed Circuit Board
TMBP	Tetramethyl Biphenyl Epoxy
DSC	Differential Scanning Calorimetry
TMA	Thermal Mechanical Analysis
DMA	Dynamic Mechanical Analysis
FTIR	Fourier-Transform Infrared Spectroscopy
Al (III) acac	Aluminum (III) Acetylacetonate
Cu (II) acac	Copper (II) Acetylacetonate
Cu (II) bzac	Copper (II) Benzoylacetonate
α_1	Coefficient of Thermal Expansion in Glassy Region
α_2	Coefficient of Thermal Expansion in Rubbery Region
G’	Storage Modulus
$T_{5\%}$	Temperature at 5% Weight Loss
$T_{10\%}$	Temperature at 10% Weight Loss
T_i	Initial Decomposition Temperature
T_p	Peak Decomposition Temperature
NCE	Novolac Type Cyanate Ester

SUMMARY

The power electronics industry has been actively seeking encapsulant materials that can serve in harsher environments. For example, with the power semiconductors leading into SiC era, the higher operation temperature (250 ºC) have proposed great challenges on the packaging materials especially on epoxy molding compound (EMC) technologies, since the temperature exceeds the stability limit of typical epoxy (EP) chemistry. In this thesis, EP/triazine system was selected to develop high temperature stable resin system that can meet the temperature requirement of next generation power electronics packaging.

In the first part of the thesis, different approaches were discussed to enhance the high temperature performance of a previously studied cyanate ester (CE)/ biphenyl EP blend which is impaired by the hydrolysis degradation of remaining cyanate groups. Firstly, the effects of different metal catalyst on the CE properties were discussed. Secondly, a triazine containing molecule triglycidyl isocyanurate (TGIC) was employed to increase the triazine content without increasing CE feed ratio to circumstance problem of unreacted cyanate groups. Finally, the high heat resistant novolac type CE was employed to form the NCE/EP blend, and their blends with different feed ratio were systematically evaluated.

In the second part, a detailed characterization of a high heat resistant CE/novolac type EP blends and the investigation on their degradation under long-term high temperature storage were summarized. The effects of the CE concentration on the thermomechanical properties of the copolymer were explored, where a tradeoff behavior between the triazine content and crosslink density was accounted for the property change. In addition, the

distinguished thermal degradation mechanisms in copolymer with different compositions were identified and illustrated. The knowledge obtained in this work can serve as a reference in the future to formulate EP/triazine based resin system for high temperature applications.

CHAPTER 1. INTRODUCTION

This chapter is devoted to introducing the background and the motivation on developing epoxy (EP)/triazine based resin system for high temperature encapsulants applications. It will first provide a brief overview of the current trends in power electronic packaging technologies and the next set of challenges, specifically focused on the growing demands on encapsulation materials to serve at harsher environments. The review of epoxy molding compound (EMC) materials and the high temperature stable resin chemistry were given after that. This is followed by an overview on the research works as well as industrial efforts on developing cyanate ester/ epoxy (CE/EP) copolymer chemistry for high temperature applications. Finally, the research objectives of developing high temperature stable resin system for EMC and the approaches will be discussed.

1.1 Trends in Power Electronics Packaging

Power electronics refer to the electronic components functioning the control and conversion of electric power [1]. In recent years, we have seen rapidly increasing demands in the power electronics markets in almost all application areas including communication devices, entertainment, computing, automotive and industrial power supplies [2]. Especially, with the trend of developing electric vehicles/ hybrid electric vehicles (EV/ HEV) in the automotive industries to utilize clean electrical energy in powering vehicles, the power control and conversion units including inverters and converters are gaining increasing importance [3].

Progresses in the power semiconductor industries in the past decades were mainly made toward higher power density of the power module to meet the needs of advanced features and higher efficiencies. As a result, higher requirements were proposed on the high-performance power packages to align with the increasing power, increasing design complexity and the decreasing margin size of the power devices. The packaging of the power electronic devices involves the solutions to electrical, thermal and mechanical problems, and will gain complexity with higher degree of integration. In the simplest form, a discrete power package will include the power die (for example metal-oxide-semiconductor field effect transistor (MOSFET)s and insulated gate bipolar transistor (IGBT)s), solder paste for die attach, lead frame and pad, bond wires and epoxy molding compound (EMC) as encapsulation, seen in Figure 1.1.1 [1]. Other types of encapsulant for high power applications include glass, hydroset ceramics and other types of polymeric materials including silicone and polyimide. Here the silicone gel have also been widely applied as encapsulation in power electronics, however their high coefficient of thermal expansion (CTE) mismatch with the substrate the the chips and their stiffening behavior at elevated temperature limited their use in high temperature applications [4].

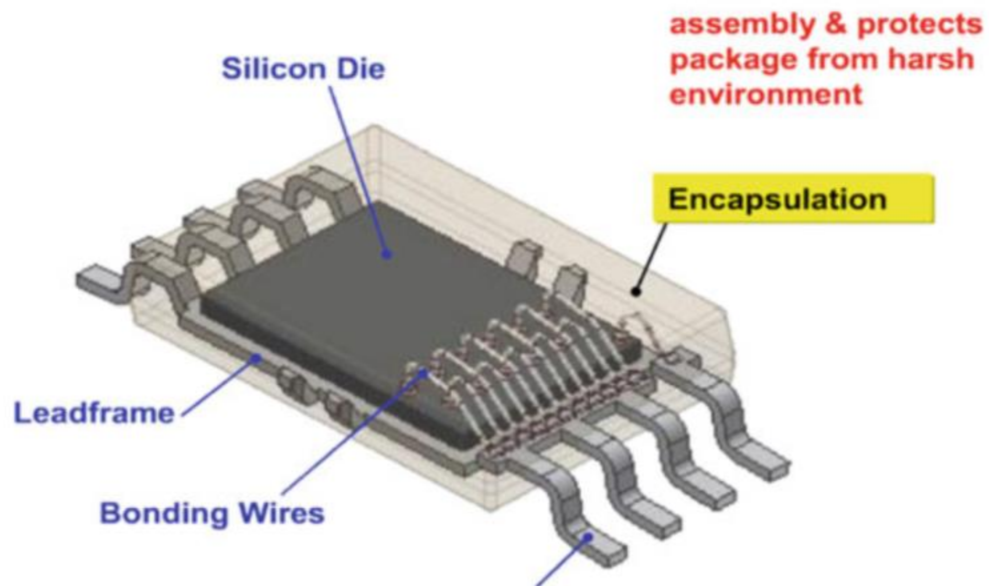

Figure 1.1.1 The structure of a typical power package SO-8 [1].

The different power packages originate from different device integrations. The current integration methods of the power devices can be separated into two major modes: monolithic integrations and hybrid integrations. The monolithic integrations are defined as the integrated circuit (IC) constructed on a single piece of semiconductor materials that will lead to the system on chip (SOC) packaging design, and the hybrid integrations are ICs contains multiple chips interconnected together and carried by ceramic substrate which requires the system in package (SiP) design. Currently, 3D heterogeneous integration will be the trend of monolithic integration while the more flexible hybrid design will be pursuing higher switching frequency with reducing the bulky magnetics and capacitances for high efficiency and low harmonics [1].

As an important growing power, it is noteworthy that the silicon carbide (SiC) and other wide band gap (WBG) semiconductors will be important supplements or even replacements to the current silicon technology for high power applications in the hybrid integrations due to their superior dynamic characteristics, overload capability and electrical/ thermal performances [5-7]. To be more specific, their advantages include:

(1) The SiC possess a much higher breakdown voltage than Si. This can allow a thinner drift region to be designed which will result in a lower specific on-resistance. The majority carrier device including MOSFET and Schottky diodes can thus be employed.
(2) Higher switching frequency can be used due to the greatly reduced switching loss in the majority carrier device.
(3) The large bandgap leads to lower intrinsic carrier concentration and higher junction temperature. For example, the SiC devices can work at 500-550 ℃, while the maximum of silicon devices will be below 200 ℃.

However, high performance of the WBG semiconductors proposes greater challenges on the packaging [1, 2, 8]. To ensure the lifetime reliability of the package, the thermal stability of the encapsulation materials is a key issue. Typical EMCs will show early failure under temperature higher than 180 ℃ due to their low glass transition temperature (T_g) and their weak backbone chemistry under thermo-oxidative environment [4, 9]. Therefore, the development of robust materials to encapsulate the SiC chips is of great importance to unleash the power of future SiC devices.

1.2 Overview of Epoxy Molding Compound

Molding compound technology has a long history over several decades in electronic packaging industry. It is usually the outermost encapsulation in electronic packages to protect the electronic system from internal and external forces including short circuiting, dust, moisture as well as impact and pressure during assembly and service [10]. An example of EMC is given in Figure 1.2.1. To meet the serving and processing requirements, the molding material should offer high toughness, good adhesion to the substrate, high electrical resistivity, low processing viscosity, fast-cure behavior, and flame retardancy. EP resin are known to provide good adhesion, good processability, low cost along with versatile curing chemistry, and thus is the standard polymer resin used in molding compound [10, 11]. Typically, the EMC contains 5-10 % of EP resin, ~ 5 % of hardener resin, 70-90 % of fused silica filler and other additives including coupling agent, flame retardant and colored agent, etc. The main function of the high loading of inorganic fillers in EMC is to decrease the CTE to better match with that of the substrate and to decrease the moisture absorption.

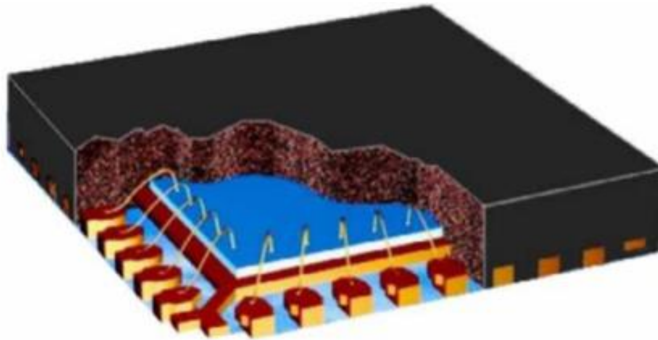

Figure 1.2.1 Example of EMC in a package [10].

The methods of applying EMC mainly include the traditional transfer molding and the compression molding [10], the procedures are as shown in Figure 1.2.2. In the transfer

molding process, the substrate, lead frame and interposer with silicon chip is placed in the mold cavities. The molding compound is then injected into the closed mold under pressure. Molded package will be released after EMC cured. The moldability of the EMC represent its ability to flow to occupy the empty space in mold cavity and is important perimeter for molding quality. The compression molding on the other hand do not involve the injection process into a close mold. The EMC is placed on the bottom of the mold and melt by thermal input. Compression of the part to be molded are then compressed into the EMC and released after EMC curing under temperature and pressure. The compression molding is gaining popularity since its characteristics including the reduced materials waste including cull and runner, the ability to control molding pressure and to accommodate package thickness [12].

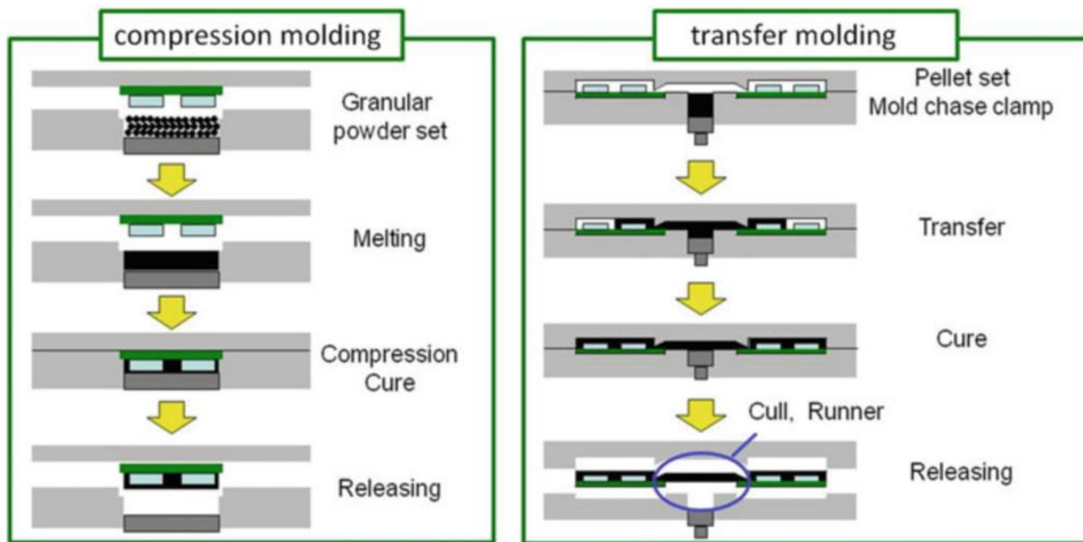

Figure 1.2.2 Comparison of molding method [10].

The molding compound is the standard encapsulation technology used in the discrete power packages since its very start and has also been widely used in power ICs.

Although there is trend to eliminate the use of EMC as encapsulation materials in the advanced MOSFET package design (MOSFET BGA (Ball Grid Array) or WL-CSP (Wafer Level- Chip Scale Package)), EMC could still serve as remolded substrate components and will gain increasing importance in the future power electronics packaging technology due to its enhanced handling and mechanical robustness [1]. To meet the requirements of the next generation power electronics with the advancing in WBG power semiconductor technologies, new EMC material with enhanced thermal stability is to be developed to withstand a much higher temperature than the current Si based devices.

1.3 Criteria and Approaches on High Temperature Polymeric Material

Thermal stability of the EP resin in EMC is critical to ensure the electrical and mechanical reliability of a power package. The parameters to describe the thermal stability of a polymer material is rather comprehensive. From a first notice, the T_g is an important measure of the dimensional stability of the polymer during heating and cooling. From an electronic packaging standpoint, the CTE mismatch between EMC and Si or substrate is the origin of delamination at the interface which can cause package failure [13]. This mismatch would become more severe at over T_g due to the freed chain motion in the resin leading to a much larger CTE [14, 15]. Conventional EP chemistry generally gives a T_g below 180 ºC and thus cannot support the operation of WBG devices [4, 16]. A high T_g material is preferred to suppress the thermal expansion or the oxidative degradation kinetics of EMC at high temperature.

Other than that, the thermal gravimetric analysis (TGA) is a useful tool to determine the weight loss behavior of the material in a short-term manner, and it can be performed

under different atmosphere to separate the thermal degradation and thermo-oxidative degradation [17-19]. Higher decomposition temperature indicates a better thermal stability when exposed to elevated temperature. A mass spectrometric study is usually associated with the TGA to determine the decomposition products. Besides, the heat distortion temperature (HDT) measures the temperature at which the material mechanically deforms and is useful parameter in describing the physical stability under load at increased temperature [20, 21]. Beyond the short-term thermal stability, the long-term aging under high temperature of the material is an important evaluation in real packaging application. This can be classified into physical stability including physical properties (strain at break, hardness, toughness, adhesion strength, T_g etc.) stability and chemical (mass, chemical structure) stability [22-25]. The combination of the above-mentioned properties determines the overall ability of material to resist high temperature.

Various types of chemical reaction can occur during the high temperature storage and cause different property changes of the resin. For example, although further curing could take place during the high temperature aging that lead to increase in T_g and modulus, when exposed to high temperature (especially when higher than T_g of the resin) in air for a prolonged time, the EMC will deform and crack and lead to package failure [26, 27]. Generally, breakdown of the EMC mainly happens in the EP resin part that is less thermally stable compared to inorganic filler. Typical EP chemistry including bisphenol type, biphenyl type and novolac type etc. cured with amine, anhydride or phenolic resin were not able to survive at temperature over 200 ºC in air where they suffer from the severe thermo-oxidative degradations. During this period, random chain scission will occur at the weak linkages releasing small volatiles and generating free radicals at chain ends. The free

radicals can attack other polymer chains to assist the chain scission, and the reactive chain ends can form coupling or disproportionation when meeting other radical chain ends, where the coupling causes further crosslinking and lead to brittleness while disproportionation causes the breakdown of backbone structure. The radical gains much higher reactivity when reacted with the oxygen diffused into polymer bulk to form peroxyl radicals and facilitate the degradation process [28, 29]. Water molecules absorbed by the EP add complexity in the high temperature degradation of the resin which can induce the hydrolysis degradation or the plasticizing effects [30, 31]. To resist these degradations at high temperature, structurally and chemically more robust polymer backbone needs to be developed.

Traditionally, the EMC used for high temperature applications were based on EPN (epoxy phenol novolac) or ECN (epoxy cresol novolac) resin cured with hydroxyl phenolic resin. The high aromaticity and average functionality of these molecules will generally lead to a higher crosslinking density and thus the higher T_g [32, 33]. However, difficulties in achieving T_g over 200 ºC were still found and the long-term aging behavior was far from satisfactory. In fact, it was reported that some of the high T_g EP chemistry can lead to larger weight loss and earlier fail during aging, which was attributed to the encouraged radical attack inside the closely packed structure of these high T_g epoxies [34]. The blending of other thermally stable polymers in EP resin is another direction to approach and has also been reported in the past decades. Thermoplastics have been employed as additives in EP resin mainly for toughening purpose, including polyetherimide (PEI) [35, 36], polyethersulfone (PES) [37] and poly (ether ether ketone) (PEEK) [38], and were reported to increase T_g of high cross-link epoxies as well. Among the thermosetting polymers,

polyimide [39], bismaleimide (BMI) [40], cyanate ester [41, 42], phthalonitrile [43], and benzocyclobutene (BCB) [44] polymer are well known for their resistance to high temperature oxidative degradations. Generally, the high crosslinking density and the rigid backbone from highly aromatic structures contributes to the high temperature performance of these materials. The blends of polyimide, BMI and cyanate ester each with epoxies have been studied on chemistry and properties [45-48]. Despite their superior performance, some of the typical high temperature thermosets suffered from the high cost, high curing requirements and the brittleness of the sample due to their closely packed structure without chain extension ability [49]. CE resin is a promising candidate for the high temperature EMC application due to its balanced thermal and mechanical performance and the attracting dielectric properties. Moreover, its good compatibility with EP, easiness of handling and relative low temperature curing all benefits the formulation design with EP resin toward EMC applications.

1.4 The Development of Cyanate Ester and Epoxy Copolymer System

The approaches in high temperature stable while processable EP material has been proposed with introducing triazine functional functional groups by the direct insertion or the *in-situ* formation (CE/EP copolymerization) method. CE is a type of high temperature thermosetting material whose thermal and mechanical properties lies in between EP and polyimide resins. The curing of CE multifunctional monomer makes use of the trimerization of cyanate functional groups to form *s*-triazine structure and crosslink, and this increase of aromaticity is where the high T_g and high temperature stability come from [41, 42, 50, 51]. Besides, CE is known for its low dielectric constant, low loss and low moisture absorption which can be ascribed to the absence of polar components and the high

free volume [51]. However, although the steam resistance of CE greatly exceeds that of EP, the CE monomers are essentially sensitive to the moisture that can lead to bubble formation in the cured laminates [52, 53]. Another major drawback is that the synthesis of CE monomer generally involves the cyanogen halides and the hazard is the main cause of its relatively high price. Up to date, various different types of CE have been developed for commercial use and some of them have found great importance in electronics, aerospace and adhesives industries.

The curing of CE resin is based on the trimerization of cyanate groups to form triazine rings. One proposed mechanism of this reaction is provided by Shimp [54] where the impurity hydroxyl groups remaining in the resin attack the cyanate ester form iminocarbonate intermediates. This intermediate can then react with other two cyanate groups and form triazine rings. These phenol act as catalyst in this case and in fact very high purity CE cannot trigger the reaction alone. The mechanism of this reaction is shown in Figure 1.4.1. A typical approach of further lowering down the curing temperature is by using metal ions as catalyst. The mechanism of these metal ion is also proposed by Shimp [54] that the coordination of metal and cyanate groups gather the cyanate esters and facilitates the reaction to form iminocarbonate intermediates, as can be seen in Figure 1.4.2. Different types of metal salts including carboxylates, octoates and acetylacetonates bearing active metals ions including copper, zinc, aluminum, cobalt, etc. [55-57]. At the same time, alkylphenol as co-catalyst are commonly used as solvents for these metal salts and can also help the hydrogen transfer in the triazine ring formation.

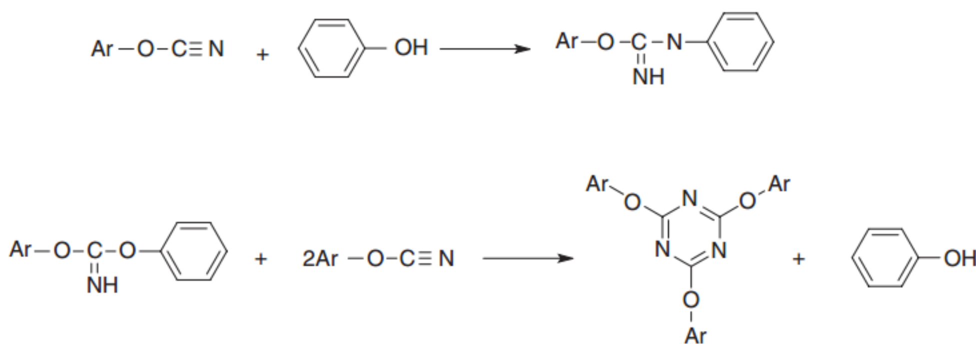

Figure 1.4.1 Reaction mechanism of CE trimerization through phenol impurities [54].

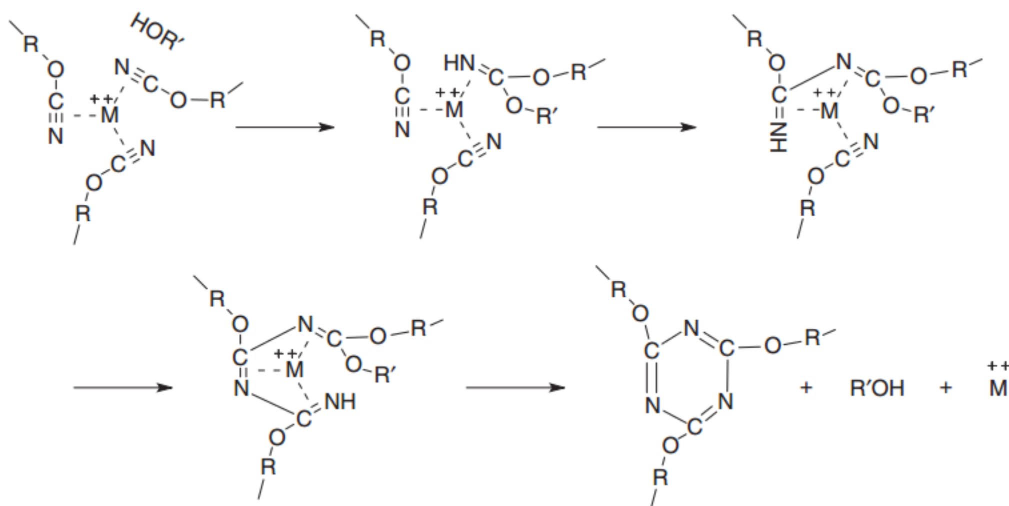

Figure 1.4.2 Reaction mechanism of CE trimerization catalyzed by metal ions [54].

EP have been commercially actively incorporated in CE to use as a solvent or to form cost effective blends. The CE and EP copolymer (CE/EP) chemistry has been studied before. The reaction route proposed by Shimp [54] include the triazine formation from trimerization of cyanate ester monomers and the copolymerization of EP and CE to form oxazolidinone, which is represented in Figure 1.4.3. The product will possess lower T_g than

pure CE but can cure at lower temperature, while exhibiting better moisture resistance properties. On the other hand, compared to amine or sulfone cured epoxies, these blends can exhibit much higher T_g and heat resistance, thus there have been approaches in improving the high temperature performance of EP resin with incorporation of triazine.

One of the first commercially important case of incorporating triazine structure in EP resin was pioneered by Mitsubishi Gas Chemical Company in 1970s [58]. They developed bismaleimide/ triazine (BT) resin for high performance substrates in printed circuit boards (PCBs) application. BT resin is made by copolymerizing bismaleimide, CE and EP resin. The mixture takes advantage of high temperature stability of both bismaleimide and CE, and the low dielectric constant and loss from the CE part. Since then, researches have been done in developing high-performance CE/EP blends and their composite materials. Large amount of information was gained, and some were converted into commercially important inventions.

Kim [59] reported the effects of CE on facilitating curing and enhancing the thermal stability of a bisphenol A EP. Lin [60] studied the curing reaction in two kinds of EP/ CE blend and proposed different reaction path ways in a bisphenol A type and a cycloaliphatic type EP system. Su and Chuang [61] demonstrated the different tendency of the triazine and oxazolidinone formation in the CE and EP blends and the resulting difference in T_g and thermal stability, where in the ortho- substituted EP triazine formation is encouraged due to the steric hindrance. Ren et al. [62] described the effect of introducing EP in commercial CE on the enhancement of both mechanical strength and moisture absorption behavior. Lei et al. [63] studied the curing reaction in imidazole catalyzed CE/EP blends

and proposed the reaction route for the two different stage of curing in the polymer/ copolymer blend.

EP or CE other than the commonly seen bisphenol A type to be blended were also proposed, exhibiting an extreme versatility of the copolymer chemistry. For example, Ren et al. [64] reported the thermal performance of a triazine bearing EP and CE blend showing high T_g and good thermal stability. Sakthidharan et al. [65] prepared azomethine functionalized CE/ EP blends, where the bisphenol building blocks in CE contain different lengths of alkyl chains and showed different thermal properties. Jayakumari et al. [66] reported the synthesis of an anthraquinone dicyanate and its copolymer with EP showing improved thermal stability to the pure EP. The novolac type resins are another type of commercially important resin material can be found in a wide range of applications, mainly benefited from its high crosslink density to yield good high temperature performance. Mathew et al. [67] studied the blend of bisphenol A CE with a novolac EP which showed two T_gs and reported the effects of oxazolidinone groups in enhancing the flexural strength. Guo et al. [68] summarized the curing chemistry and kinetics of a bisphenol A CE/ novolac EP blend and proposed a composite mechanism of triazine-EP insertion and cyanate-EP reaction, and noticed the effects of un-epoxidized hydroxyl groups in the reaction with cyanate. The novolac type CE were also found in commercial product mainly by Lonza under trade name PT resin.

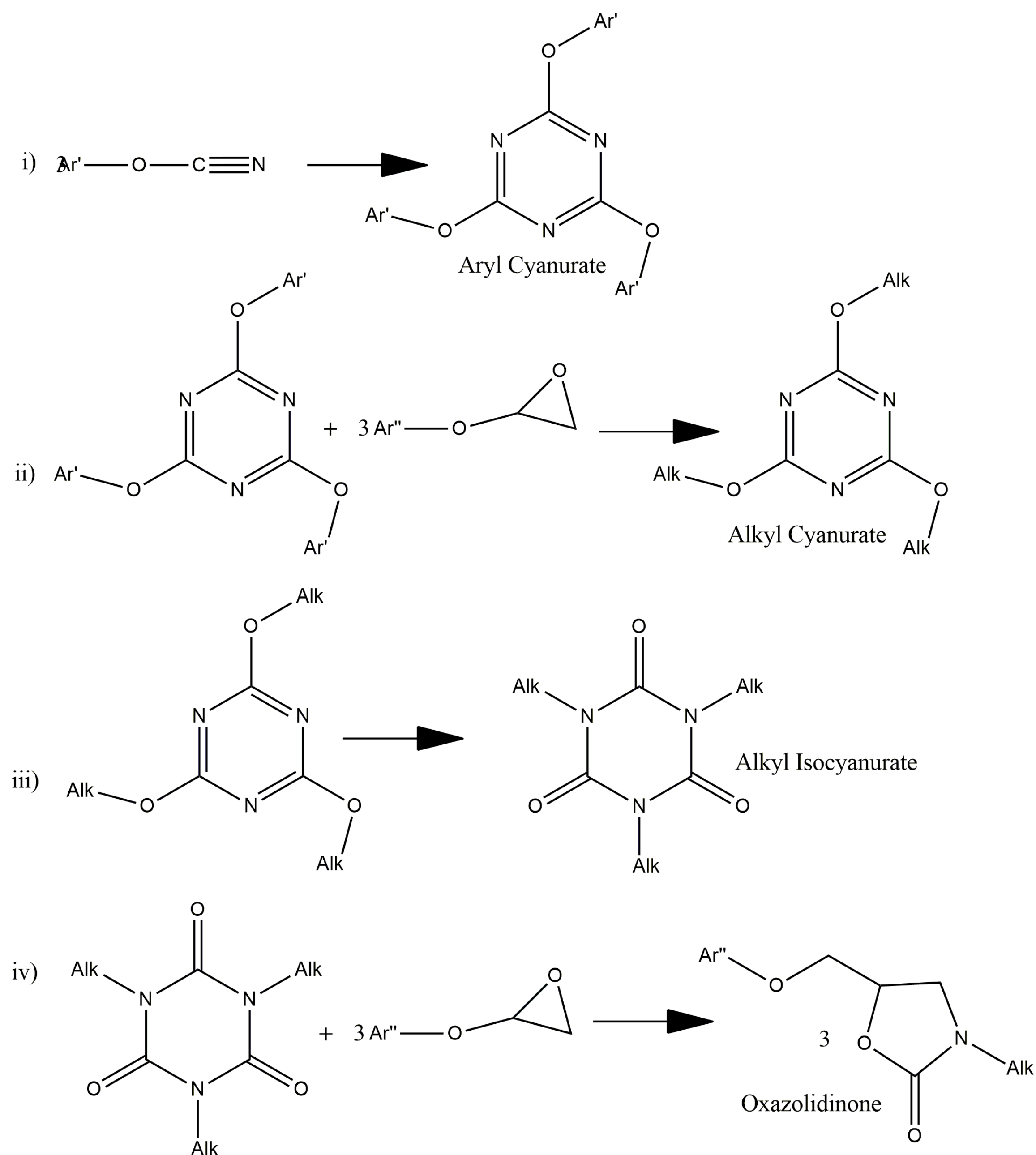

Figure 1.4.3 Schematic representation of reactions happen in a CE/EP copolymer system.

The CE/EP co-polymer system using bisphenol A type CE and biphenyl type EP with Al^{3+} catalyst has recently been explored by our group [69]. Although a higher T_g and thermal decomposition temperature were found when increasing the CE content, the

prolonged high temperature aging test showed reversed results. Higher CE concentration in the copolymer system led to larger weight loss during aging and the early fail with blistering and cracking. The severe hydrolysis degradation in CE part was believed to cause the catastrophic failure, where the carbamate can be formed during curing or aging with reaction between moisture and cyanate groups, and the decomposition of carbamate at over 190 ℃ will result in outgas of CO_2 [52, 54], as can be seen in Figure 1.4.4. Works are still needed to be done to prolong the storage life of the high T_g CE/ EP blend systems under high temperature and to further understand the nature of the high temperature degradation to demonstrate their capability for the high-power packaging applications.

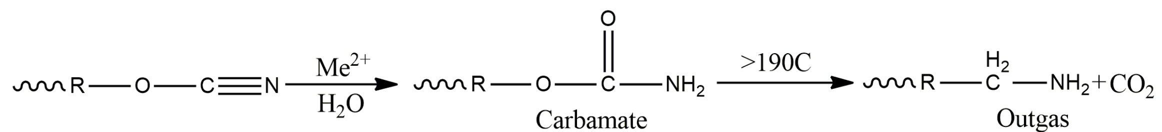

Figure 1.4.4 The reaction route of carbamate formation through the hydrolysis of cyanate groups and its decomposition that lead to out gas.

1.5 Research Objectives and Outline

The objective of this thesis is to develop high-performance EMC resin material with high temperature stability that can meet the requirements of next generation power electronics encapsulation. The utilized resin chemistry is based on CE/EP copolymer system and the work are concluded in two parts employing two types of EP components:

(1) Improving the high temperature performance of biphenyl EP/triazine system with modifications on formulation;

(2) Evaluation of novolac EP/triazine resin system and the failure analysis on high temperature storage degradations.

The results on these two research items are presented in Chapter 2 and Chapter 3, respectively.

As mentioned on the last section, the aging behavior in the CE/ biphenyl EP system was in opposite trend with Tg and thermal decomposition profiles. The hydrolysis degradation on the high CE polymers limited their application in the harsh environments. The efforts on the improving the high temperature stability of CE/ biphenyl EP system are summarized in Chapter 2. In each system, the thermomechanical properties were systematically studied. To be more specific, Chapter 2 contains following research items:

1) Studying the effects of different types of metal catalysts on the curing as well as degradation behavior of the CE polymer;
2) Studying the effects of direct insertion of triazine functional groups in the CE/EP blend;
3) Evaluating the system based on novolac type CE copolymerizing with biphenyl EP.

The novolac type resins typically give better heat resistance and flame retardancy than the typical bisphenol A or bisphenol F type, mainly due to their high functionality (which leads to high crosslink density) and larger building blocks between weak linkages (which leads to slow decomposition and better char forming). The blending of novolac type EP with CE were found in literatures [70, 71]. The Chapter 3 provides a detailed

investigation into the thermomechanical properties and aging degradation behavior of CE/ novolac EP blends. It can be divided into three parts as follow:

1) Screen test on different types of CE/ novolac EP blend, select the best combination;
2) Evaluation on a CE/ cresol novolac type EP blend system on the thermomechanical properties;
3) Study on the degradation of the CE/ cresol novolac type EP blend during aging under high temperature.

The summary and suggested work are presented in the Chapter 4.

CHAPTER 2. DEVELOPMENT AND EVALUATION ON BIPHENYL EPOXY/TRIAZINE BASED HIGH TEMPERATURE STABLE RESIN SYSTEMS

This chapter will cover the work on development of the thermally robust biphenyl epoxy (EP) formulation with the incorporation of triazine functional groups. The approaches to improve the copolymer performance include the optimization of metal catalyst, utilizing triazine containing EP and employing novolac type cyanate ester (CE) in the copolymer. The curing chemistry, thermal mechanical properties and aging degradations in these systems were systematically studied.

2.1 Materials and Experimental

Tetramethyl biphenyl epoxy (TMBP) was provided by Mitsubishi Chemical Corporation. Bisphenol A cyanate ester was purchased from Oakwood Chemical. Primaset^{TM} PT-30 resin was provided by Lonza. Tris (2,3-epoxypropyl) isocyanurate (TGIC), Copper (II) acetylacetonate, Aluminum (III) acetylacetonate and nonylphenol were purchased from Aldrich. Copper (II) benzoylacetonate were received from Eastman Organic Chemicals.

The monomers were processed in melt. The feed TMBP resins were mixed in a beaker on the hot plate at 120 ºC, with continuous stirring with magnetic stirrer. The CE monomers and the TGIC molecules (in some cases) are then poured into the melt. After vigorous stirring, the catalyst is added dropwise to the desired amount and stirred until homogenous. The catalyst is previously dissolved in the nonylphenol at elevated

temperature. Round shape samples were made by the solutions casted in the aluminium pan and cured in convection oven. These samples will be polished and cut into shape needed for testing. Before the test, samples were dried in convection oven at 100 ºC for 2 hours.

In the copolymer, all formulations were calculated based on functional group molar ratios. For example, the CE/EP 13 denotes the ratio between cyanate groups and epoxide groups was 1:3. In the second part of this chapter, the TGIC was incorporate in the CE/EP systems. All the blends kept the cyanate : epoxide ratio at 1:1 and the number in the formulation represents the percentage of epoxide groups supplied by the TGIC molecule. Metal catalyst used in the CE system is regulated by the weight percentage of active metal ion in the solution in unit ppm (parts per million), and the co-catalyst is normally counted in phr (parts per hundred resin). The Cu^{2+} were kept at 360 ppm and Al^{3+} at 150 ppm. In all studies, the nonylphenol were loaded at 3 phr.

Differential Scanning Calorimetry (DSC) was done by DSC Q2000 from TA Instrument to characterize the curing thermo profile of the polymer mix. The experiments were ramping at 10 ºC/min and were done under nitrogen atmosphere. Thermal Mechanical Analysis (TMA) was done using TMA Q400 from TA Instrument. Ramping rate was kept at 20 ºC/min and experiments were under nitrogen atmosphere. Dynamic Mechanical Analysis (DMA) was performed by DMA Q800 from TA Instrument in tension mode. Ramping rate was 3 ºC/min at oscillation frequency 1 Hz. The Thermal Gravimetric Analysis (TGA) both under nitrogen and air atmosphere used TGA Q5000 from TA Instrument. All tests programmed to ramp 20 ºC/ min to 800 ºC. Dielectric properties of the sample were tested by Agilent E4991A RF Impedance Analyzer. Fourier-Transform

Infrared spectroscopy (FTIR) was done by Thermo Scientific Nicolet iS5 FT-IR spectrometer using a diamond ATR mode. The rheology studies were performed on a Discovery HR-2 from TA Instrument with 25 mm Aluminum parallel plate. The test were done in temperature ramp mode at 5 ºC/min. Strain was kept at 1% and oscillation frequency at 1 Hz. The high temperature aging test was done in Fisher Scientific 825f convection oven and the moisture absorption done in MicroClimate bench top environmental chamber from Cincinnati SubZero Inc.

2.2 Metal Catalyst Optimization and Curing Reaction Study in Cyanate Ester/ Epoxy System

The previously studied CE/EP system with Al^{3+} catalyst was found to cause early fail in the high CE content polymers [69]. The carbamate formation reaction is known to be catalyzed by the metal chelates [54]. Certain types of metal catalyst for example zinc and titanium salts and were known to facilitate the hydrolysis reaction and are thus to be avoided. In this section, a study on the effects of different metal ions with different ligands on the CE properties is presented.

The curing of uncatalyzed CE requires substantially high temperature, as shown in the DSC scan Figure 2.2.1. The onset of curing reaction exotherm reached over 250 ºC, which is incompatible with the molding process. To facilitate the trimerization, metal salts were selected to act as catalyst. As mentioned before, the role of these metal chelates in the CE polymerization is through the chelating and gathering together cyanate groups to facilitate the trimerization process.

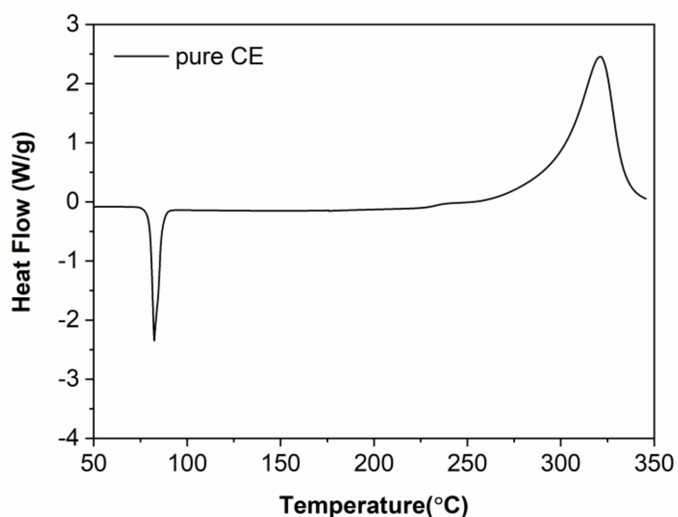

Figure 2.2.1 DSC thermogram of uncatalyzed CE.

The effects of different types of metal chelates as catalysts for CE system were investigated regarding their effects on curing and thermal properties of the cured resin. The metal chelates selected here are aluminum (III) acetylacetonate (Al (III) acac), copper (II) acetylacetonate (Cu (II) acac) and copper (II) benzoylacetonate (Cu (II) bzac), and their structures are shown in Figure 2.2.2. The electrons on the acetylacetonate or the benzoylacetonate are delocalized and can associate with metal ion to form chelation bond. When dissolved in CE, the equilibrium will be pushed towards disassociation of the compound due to the chelating force between abundant cyanate groups and metal ion. The cyanate groups brought together by these metal ions are later triggered by heat to react with hydroxyl groups and trimerize.

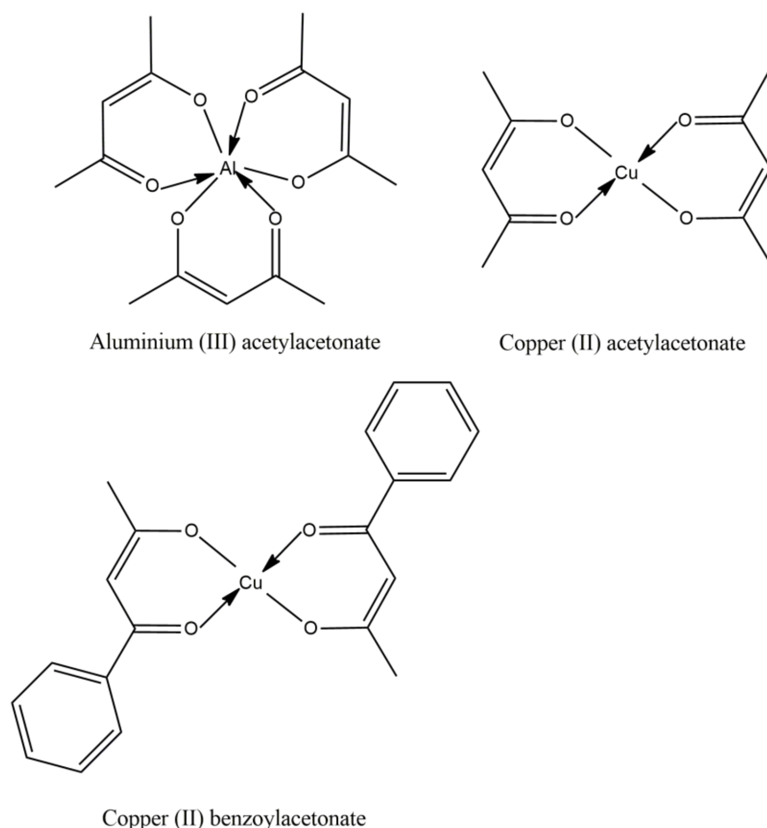

Figure 2.2.2 Chemical structure of Al(III) acac, Cu(II) acac and Cu(II) bzac.

The curing behaviour of CE under different type of metal chelates at same molar ratio (150 ppm Al^{3+} and 360 ppm Cu^{2+}) are shown in Figure 2.2.3. All three kinds of catalyst were able to greatly reduce the curing onset temperature of CE, while the Cu^{2+} ions showed higher catalysing power than Al^{3+} ion which may be due to a stronger coordination between Cu^{2+} ion and cyanate groups. A broader exothermic peak was also found in the Cu (II) catalysed cases. Comparing the Cu (II) acac and Cu (II) bzac catalysed polymers, a slightly higher temperature is required for curing reaction to take place in Cu (II) bzac case. This might be due to the steric effects as well as the resonance effect of the different ligands. The phenyl groups in bzac ligand provides steric hindrance for Cu^{2+} ion to interact with cyanate groups. They also tend to be strong π- electron donor, which caused a higher

electron density between the two coordinated oxygen atoms and thus a stronger bonding to the Cu^{2+} ion [72]. A higher temperature is required to disassociate the Cu^{2+} ion from bzac ligand in this sense.

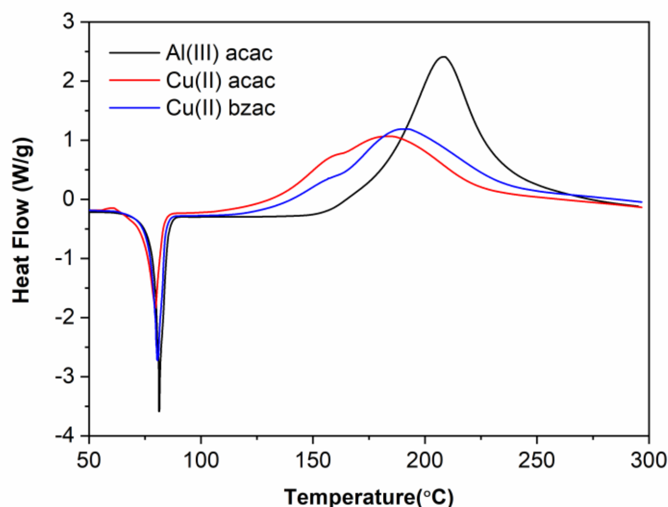

Figure 2.2.3 DSC thermograms of CE catalyzed by Al(III) acac, Cu(II) acac and Cu(II) bzac.

The FTIR spectra of the CE cured with different metal ions is shown in Figure 2.2.4. It has been reported that the carbamate groups may be formed during curing conditions when moisture is present, and this reaction could also be facilitated by the metal catalyst. Other than the appearance of triazine absorption peaks (1592 cm^{-1} and 1360 cm^{-1}) seen in all three cases, the weak peaks related to the carbamate carbonyl can also be found at 1660 cm^{-1} [73]. It can be thus inferred that the hydrolysis of cyanate groups may already take place during curing condition in presence of moisture. The intensity however differs when employing different metal chelate as catalyst, indicating their tendency to accelerate the cyanate conversion.

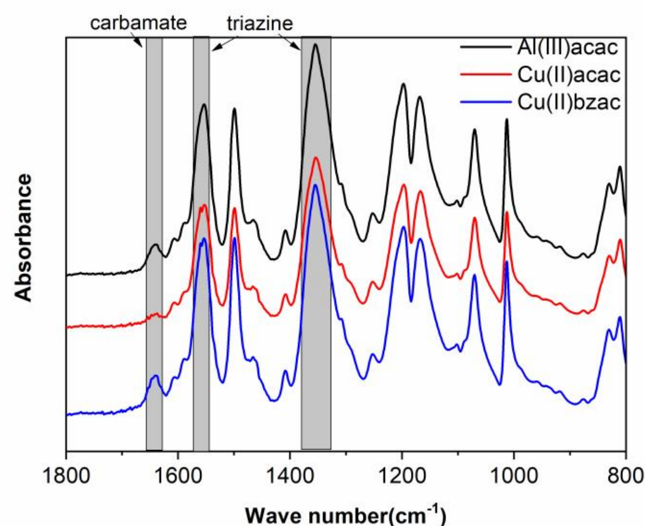

Figure 2.2.4 FTIR spectra of CE cured with Al(III) acac, Cu(II) acac and Cu(II) bzac.

The effects of these different metal ions on the cured resin properties were also demonstrated. Figure 2.2.5 shows the thermal decomposition profile of the cured CE with different catalyst. The properties extracted from TGA plots are shown in Table 2.2-1. The heat resistance properties of the CE cured by different metal catalyst were not significantly differed from each other though the Cu (II) acac cured one showed slightly better performance.

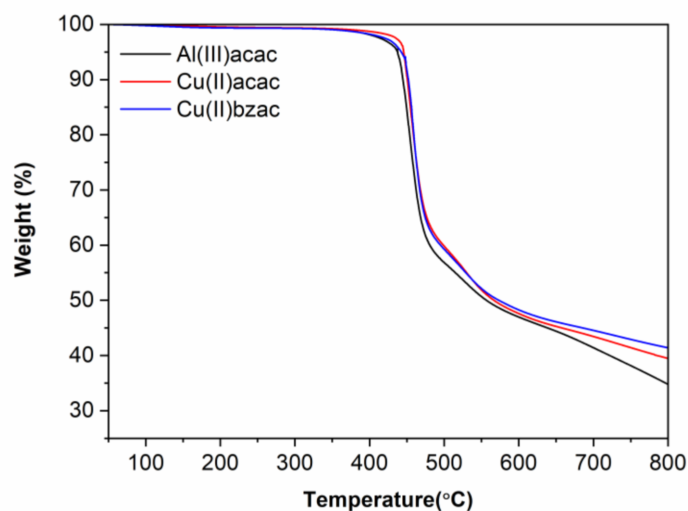

Figure 2.2.5 TGA thermogram of CE cured with Al(III) acac, Cu(II) acac and Cu(II) bzac, in N_2.

Table 2.2-1 Parameters from TGA thermogram of CE cured with Al(III) acac, Cu(II) acac and Cu(II) bzac in N_2, including the temperature at 5% and 10% weight loss and residue weight at 800 ºC.

Sample cured by	$T_{5\%}$	$T_{10\%}$	Residue at 800 ºC
Al (III) acac	437.53	444.5	34.87
Cu (II) acac	445.65	450.4	39.48
Cu (II) bzac	442.46	451.92	41.43

The glass transition temperature and CTE of the samples with three types of metal catalysts are summarized in Table 2.2-2. A high TMA T_g over 250 ºC was present for all polymers and the α_1 CTE at ~90 ppm/ºC which is typical for thermosetting polymers.

Table 2.2-2 TMA thermomechanical properties of CE cured with Al(III) acac, Cu(II) acac and Cu(II) bzac, including the T_g and CTE before and after glass transition.

Sample cured by	TMA T_g/ºC	α_1/(ppm/ºC)	α_2/(ppm/ºC)
Al (III) acac	257.85	98.91	201.1
Cu (II) acac	260.82	93.4	215.1
Cu (II) bzac	256.61	94.64	221.7

The most dominant effects of the active metal catalyst for curing CE is on their thermal stability over long term high temperature storage tests. As shown in Figure 2.2.6, the sample cured by three different catalyst exhibited similar weight loss profile in the first 500 hours under 200 ºC, while the Al (III) acac cured sample experienced drastic weight drop after 500 hours. The severe swelling and crack that led to failure was found to be the main degradation characters during aging, which was suspected to be the product of decomposition of carbamate groups within the resin. The higher intensity of carbamates seen in the Al^{3+} catalyzed materials correlates well with their early fail behavior, and it can be concluded that Cu (II) is more suitable a catalyst for curing CE. This is in accordance with the knowledge in US patent files by Shimp [56].

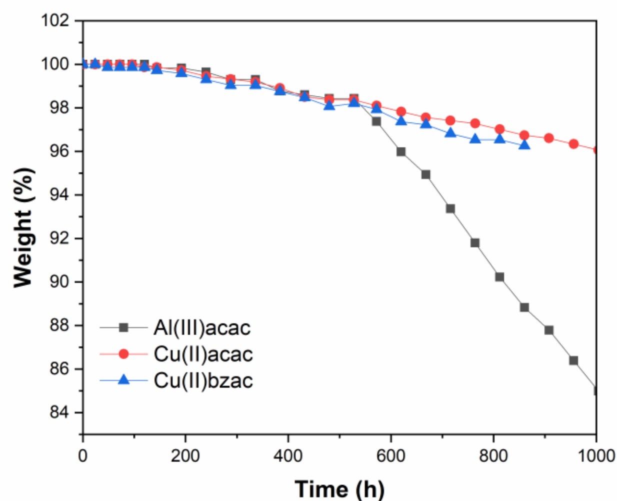

Figure 2.2.6 Weight loss profile of CE cured with Al(III) acac, Cu(II) acac and Cu(II) bzac under storage at 200 ºC.

The curing studies of the CE/EP copolymer (1:1 molar ratio) using different catalyst were conducted. The curing thermogram of the neat CE/EP, the Al^{3+} catalysed CE/EP and the Cu^{2+} catalysed CE/EP were shown in Figure 2.2.7. Similar to the pure CE/ metal chelate system, lower onset temperatures of curing were found after adding metal chelates compared to uncatalyzed case. However, although the curing thermogram of CE was similar when comparing different metal chelates, the copolymer showed differed behaviour. Two separate curing peaks were clearly evidenced in Cu^{2+} catalysed polymers. Of these two curing peaks, the first exotherm exhibited an onset of around 150 ºC which resembles the curing of pure CE, while the onset of the second one was at 225 ºC. The origin of these two distinctive peaks were explored by means of in-situ FTIR spectroscopy assisted by the DSC isothermal tests.

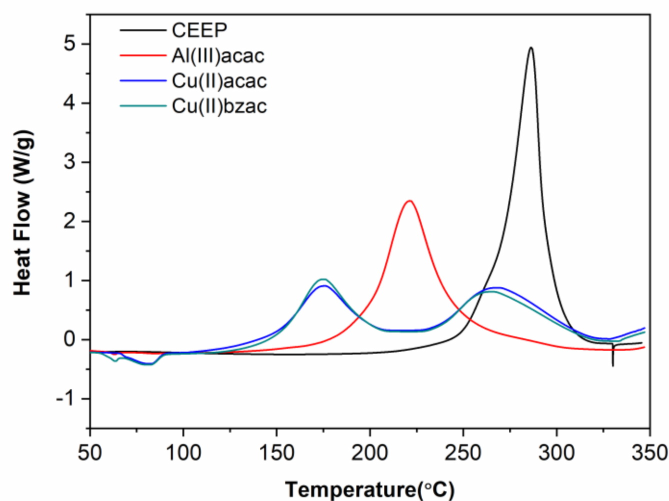

Figure 2.2.7 DSC curing thermogram of pure CE/EP blend and its mixture with Al(III) acac, Cu(II) acac and Cu(II) bzac.

The evolution of chemical structures in the Cu^{2+} catalysed CE/EP blend during the dynamic DSC scan was depicted in Figure 2.2.8. At the onset of first curing exotherm, the clear characteristics of cyanate groups were present at ~2250 cm^{-1} as well as the epoxide groups at 915 cm^{-1}. Exothermic reactions took place during further heating. An increase of triazine peak (1536 cm^{-1} and 1360 cm^{-1}) intensity and a decrease of the cyanate groups intensity indicates the reaction of the cyanate trimerization. At the end of the first curing exotherm at 200 ºC, the conversion of cyanate groups was complete and no peak at 2250 cm^{-1} could be found. However, the peak corresponding to epoxide groups remained unchanged during the first exotherm. With temperature ramped over 200 ºC, the intensity of both the epoxide groups and triazine decreased, while the growth in the oxazolidinone (1743 cm^{-1}) peak became apparent. The above-mentioned changes in the chemical structure during temperature increase illustrated the curing reactions happened in two curing

exotherms seen in the Cu^{2+} catalyzed CE/EP blend. During the first exotherm, trimerization of the CE took place with consuming the cyanate groups and forming triazine functions; the higher temperature exotherm relates to the insertion of epoxied groups in triazine rings and the reformation of oxazolidinone (see step ii-iv in Figure 1.4.3). These two competing reactions were proved to be temperature selective, as seen from the studies in the DSC isothermal tests.

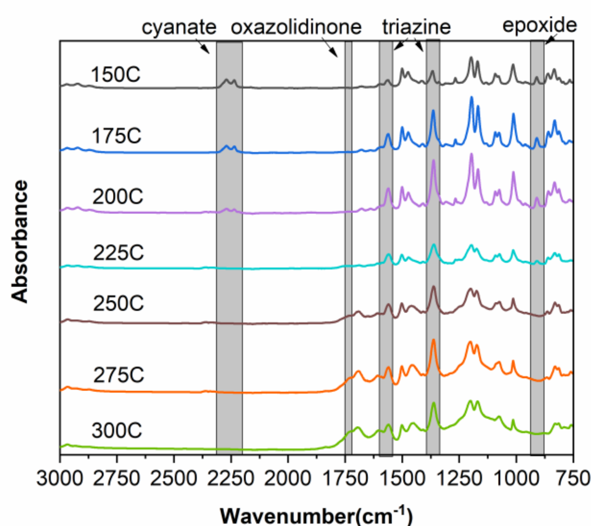

Figure 2.2.8 FTIR spectra of CE/EP with Cu (II) acac catalyst during temperature ramp.

It has been illustrated that the triazine structure is the determining factor on the high temperature stability and T_g of the CE polymer, while the product of CE/EP copolymerization, the oxazolidinone with chain extension characteristics could contribute to the sample fracture toughness while is less thermally stable. Since the second exotherm in the curing of CE/EP was to consume the triazine rings, it could be favorable if controlling the curing schedule to preserve the triazine structure and limit the copolymerization. In this

case, even in low CE to EP ratio, a high stable triazine part support the high temperature performance, while the remaining epoxide groups can possibly go through etherification reactions to crosslink and provide adhesion to substrates. However, from the isothermal DSC tests it revealed that the thermodynamics of the two reaction requires triggering by certain thermal conditions where full cure cannot be achieved until reaching certain temperature.

2.3 Direct Insertion of Triazine Functions in Cyanate Ester/ Epoxy system

To alleviate the problem of high temperature storage failure in high CE content blends while exploit the benefits of the rigid triazine structure, it is worth studying to keep the CE concentration low in the copolymer system while incorporate triazine functions by direct insertion. Other than the *in-situ* formation of triazine rings, it has been known that EP or hardener molecules containing triazine structures can also benefit the high temperature performance. For example, the triglycidyl isocyanurate (TGIC) which is an isocyanurate ring bearing three glycidyl type epoxide groups has been employed by powder coating industry for improving durability of the EP coating materials [74]. The triazine structure and high functionality results in high heat resistance and high crosslinking density. Here the TGIC was used as a supplementary epoxide source for the previously used biphenyl EP. Note that the molar ratio of epoxide groups to the cyanate groups were kept at constant at 1:1.

The effects of TGIC on curing of CE/EP copolymer system was investigated. DSC thermogram (Figure 2.3.1) depicted similar profile for the TGIC added polymers showing two distinguished exothermic peaks, which as mentioned before correlates to the CE

trimerization and the CE/EP copolymerization, respectively. It could be found that with higher concentration of TGIC, the onsets of the second curing exotherm was gradually decreasing, which implies a lower kinetic barrier benefitted from higher functionalized TGIC molecule compared with TMBP. At the same time, the amount of heat released during the copolymerization reaction were reduced. This might be due to the steric hindrance of the trifunctional molecules to the epoxide insertion on formed triazine rings that limited the ring opening of epoxides.

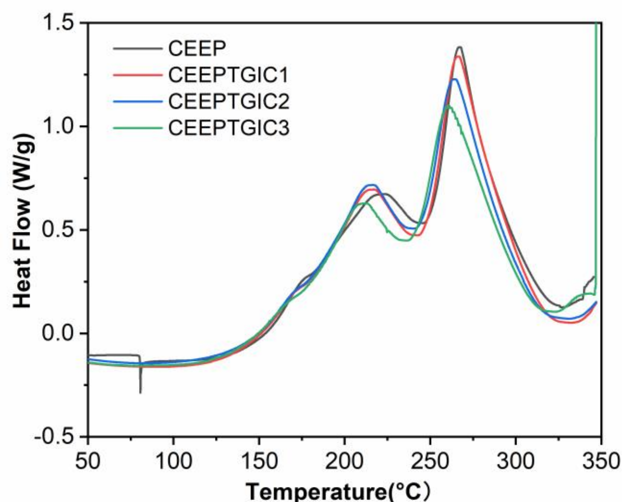

Figure 2.3.1. DSC curing profile of CE/EP and TGIC incorporated CE/EP.

The FTIR spectra in Figure 2.3.2 illustrates the effects of replacing part of the TMBP by TGIC on the sample chemical structures. An increasing intensity can be seen in both the isocyanurate (1692 cm-1) and the triazine functions with increasing concentration of TGIC molecules. The introduction of triazine structure by means of direct insertion of TGIC was confirmed.

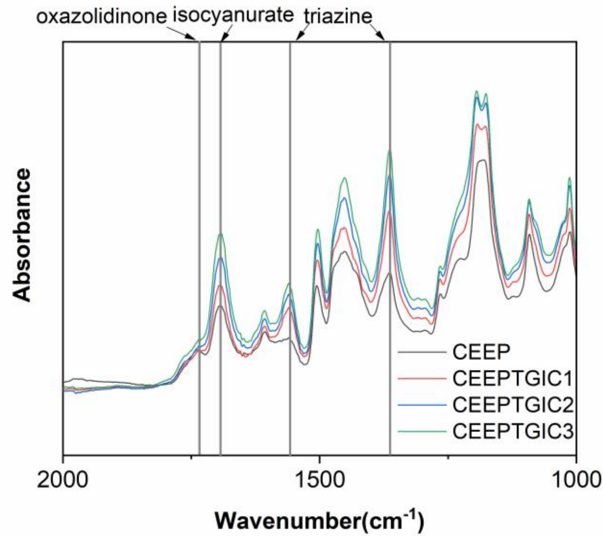

Figure 2.3.2. FTIR spectra at 1000 cm^{-1} to 2000 cm^{-1} region of cured CE/EP and TGIC incorporated CE/EP.

The T_g of the TGIC added CE/EP system were determined by TMA and DMA. The TMA results of the copolymers are summarized in Table 2.3-1. A clear trend of increasing T_g was observed from 218.53 ℃ to 237. 14 ℃ when adding TGIC molecules. Moreover, the decreasing α_2 CTE, which describes the reduced thermal expansion at rubbery state implies a higher crosslink density of the sample, benefitted from the introduction of trifunctional TGIC epoxies. On the other hand, the rigid backbone structure reinforced by triazine rings confines the relieve of chain motions during glass transition and thus increase the T_g.

Table 2.3-1 Parameters from TMA tests on cured CE/EP and TGIC incorporated CE/EP, including the T_g and CTE before and after glass transition.

Sample	TMA T_g/ ºC	α_1/ ppm/ ºC	α_2/ ppm/ ºC
CEEP	218.53	58.94	221.41
CEEPTGIC1	216.64	53.44	213.62
CEEPTGIC2	231.42	60.31	200.05
CEEPTGIC3	237.14	70.71	181.33

The DMA tan δ profiles of the CE/EP and the samples with TGIC added are shown in Figure 2.3.3. A first increase and then decrease in the T_g and decrease in damping were evidenced. The analysis on the storage moduli (G') of these samples and the calculated crosslink density (shown in Table 2.3-2) indicated the increase in crosslink density of the TGIC incorporated CE/EP bend, which correlates well with the TMA analysis. The calculation of crosslink density from rubbery modulus followed the formulation described in [75]. Like the above-mentioned mechanism, further adding the TGIC molecules to replace TMBP may cause the plasticizing effects from the unreacted small molecules, and the T_g can rather drop in this sense.

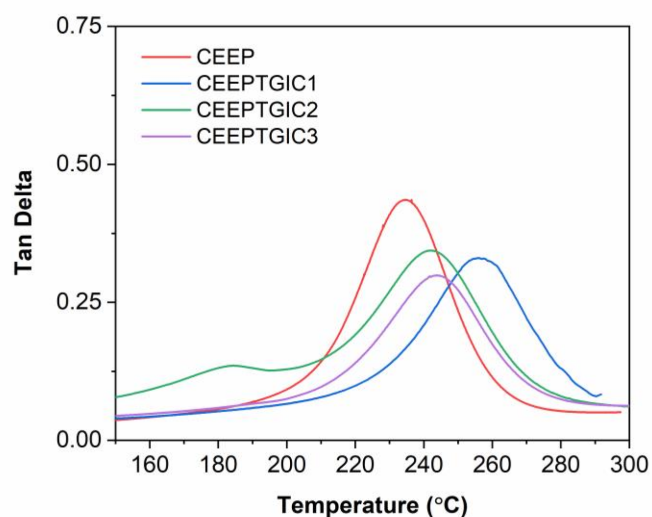

Figure 2.3.3. DMA tan δ profiles of CE/EP and TGIC incorporated CE/EP.

Table 2.3-2 DMA thermomechanical properties of CE/EP and TGIC incorporated CE/EP, including T_g, storage moduli at rubbery region and the calculated crosslink density accordingly.

Sample	DMA T_g/ ºC	G' at 30 ºC above T_g / Mpa	Crosslink density/ 10^{-3} mol/ cm^3
CEEP	234.58	54.96	8.328
CEEPTGIC1	255.82	105.4	14.785
CEEPTGIC2	241.91	82.96	12.232
CEEPTGIC3	243.52	109.2	16.007

The thermal decomposition behavior of the samples was evaluated in both N_2 (Figure 2.3.4) and air atmosphere (Figure 2.3.5). The properties were extracted to show in Table 2.3-3. As clearly denoted in the magnified view in the Figure 2.3.4 and the $T_{5\%}$, $T_{10\%}$ data in the table, a higher decomposition onset during the TGA ramp in N_2 was found for TGIC incorporated CE/EP up to 10 ℃, representing their high heat resistant property brought by the increase of triazine functions and increasing crosslink density. In air a two-stage weight loss was apparent for all copolymers and the decomposition onset of the samples were not distinguishable. The first stage of weight loss relates to the chain scission and releasing of small segments as volatiles and degradation while the second corresponds to the oxidation of carbonaceous residues [76]. The effects of introducing TGIC was not obvious during the first stage of weight loss. In the second weight loss period, the TGIC incorporated copolymer showed larger tendency of oxidation weight loss. This may relate to the structure of the formed char.

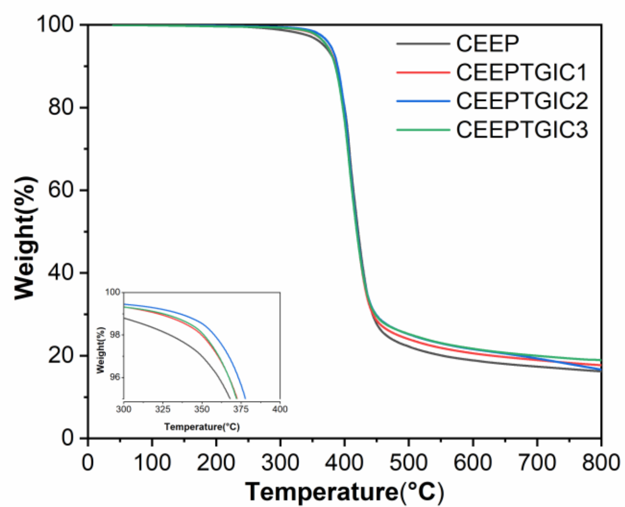

Figure 2.3.4 TGA profile of CE/EP and TGIC incorporated CE/EP in N_2 atmosphere. The inset magnifies the 300-400 ºC region.

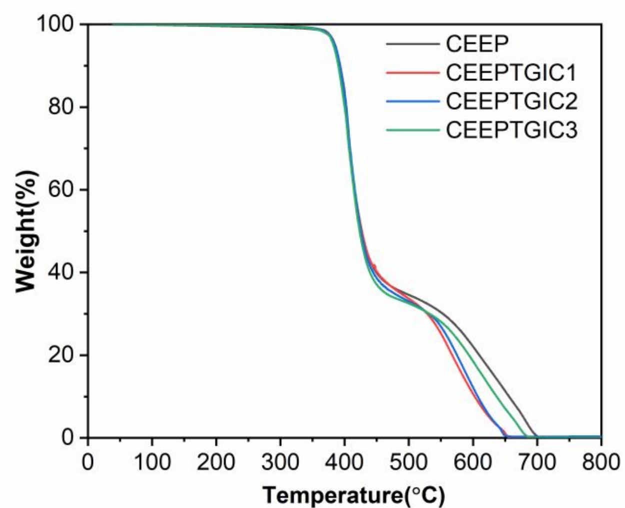

Figure 2.3.5 TGA profile of CE/EP and TGIC incorporated CE/EP in air atmosphere.

Table 2.3-3 Summarized parameters from TGA thermogram of CE/EP and TGIC incorporated CE/EP in N_2 and air atmosphere, including the temperature at 5% and 10% weight loss and residue weight at 800 ºC (in N_2).

Sample	$T_{5\%}$ in N_2 /ºC	$T_{10\%}$ in N_2 /ºC	Char Yield at 800 ºC/ %	$T_{5\%}$ in air /ºC	$T_{10\%}$ in air /ºC
CEEP	367.11	386.66	16.22	384.58	393.12
CEEPTGIC1	371.92	386.4	17.71	385.24	392.63
CEEPTGIC2	377.25	389.28	16.66	385.95	392.86
CEEPTGIC3	371.91	386.04	18.94	382.72	390.3

Despite the success in increasing crosslink density and introducing triazine structures in the CE/EP blend by using the TGIC and their intriguing feature seen in the T_g and thermal decomposition behavior, their resistance to long-term exposure to elevated temperature was not satisfying. The comparation of the weight loss of CE, CE/EP and the TGIC incorporated CE/EP during aging at 250 ºC is shown in Figure 2.3.6. An increasing weight loss gradient during the high temperature storage could be found after adding the TGIC molecules. However, compared to the dramatic breakdown of the pure CE after ~72 hours, all the sample showed better storage life. The reason of the larger weight loss of TGIC incorporated CE/EP was attributed to the higher moisture absorption in these samples, as shown in Table 2.3-4. The higher absorption of moisture during the aging on

the one hand plasticize the resin and facilitate the oxidation kinetics, on the other hand is vital in our copolymer system due to the known hydrolysis degradation of CE.

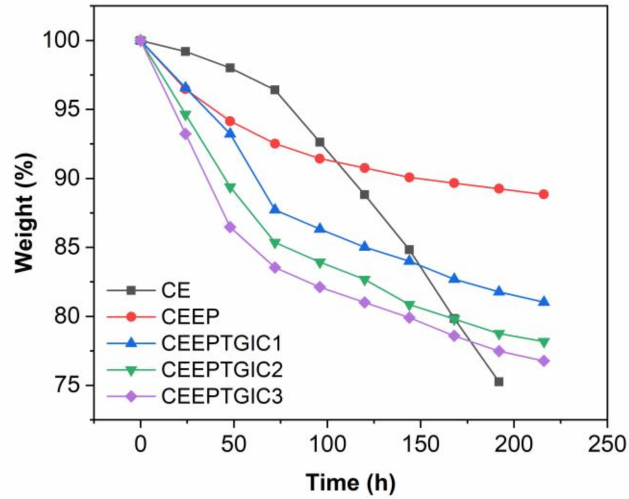

Figure 2.3.6 Weight loss under 250 ℃ aging of CE, CE/EP and the TGIC incorporated CE/EP.

Table 2.3-4 Moisture absorption of CE/EP and the TGIC incorporated CE/EP. Data was selected based on the saturation weight gain in 105 ℃/ 100 RH HAST chamber.

Sample	Moisture Absorption/ %
CEEP	1.37
CEEPTGIC1	1.41
CEEPTGIC2	1.57

CEEPTGIC3	3.40

The origin of high moisture absorption of the TGIC incorporated CE/EP was explained by the increased content of the polar hydroxyl groups in the resin that can cause sample hydrophilicity. As depicted in Figure 2.3.7, the replacement of TMBP by trifunctional TGIC introduced more aliphatic C-H seen at their stretching absorption peak at ~2950 cm^{-1} while the aromatic C-H stretching at ~3050 cm^{-1} remained similar. Larger amount of -OH groups were introduced seen at ~3300 cm-1 due to the increased ratio of other ring opening reactions of epoxides in the system as the difficulty of all participating in the copolymerization from steric standpoint as mentioned before.

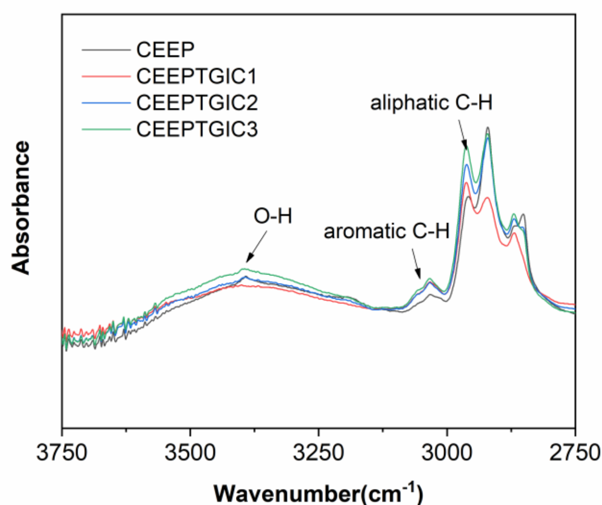

Figure 2.3.7 FTIR spectra of CE/EP and the TGIC incorporated CE/EP at 2750 cm^{-1}~ 3750 cm^{-1} region.

2.4 Development of Novolac Type Cyanate Ester/ Epoxy Copolymer System

The novolac type CE (NCE) were known to support better high temperature resistance than the bisphenol A type CE, due to the high crosslink density in the cured resins. The commercialized NCE are mostly supplied by Lonza, where they synthesized various types of NCE monomers with varied functionalities. Some of the polymers have exhibited a T_g over 400 ℃ after proper cure. The NCE used here has structure shown in Figure 2.4.1 showing a functionality of 3 in each molecule. In the below section, the copolymer system constructed by the NCE and TMBP were evaluated in detail.

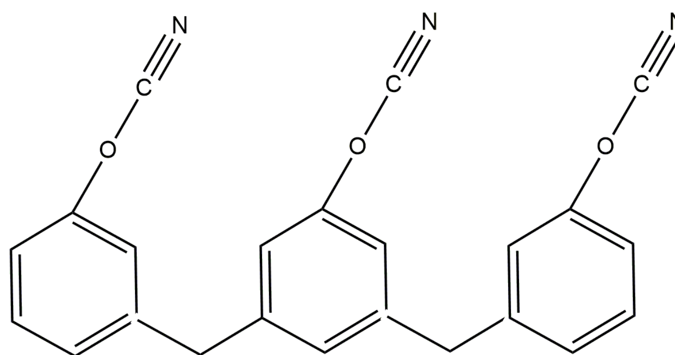

Primaset PT-30 Novolac Type Cyanate Ester

Figure 2.4.1 Structure of the NCE used in this study.

The curing profiles of the copolymers are shown in Figure 2.4.2. The onset of pure NCE was not deviated much from the bisphenol A type CE under same catalyst usage, showing an onset close to 120 ℃. And still, two separate peaks are shown in the NCE/EP blends, where with the increase of EP concentration, the onset of the first peak shifted towards higher temperature, and the area under it decreased. Opposite trend was noticed for the second curing exotherm. Therefore, it can still be inferred that the trimerization of CE took place at lower temperature while the copolymerization between CE and EP need to be triggered at an elevated temperature.

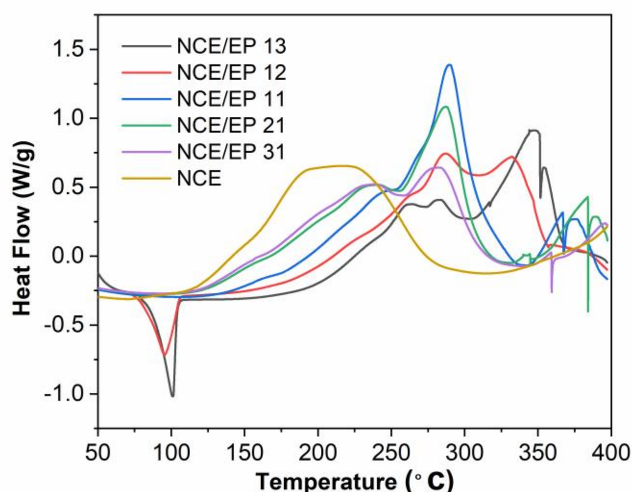

Figure 2.4.2 DSC curing thermogram of the pure NCE and the NCE/ EP blends at different ratio.

The gel behavior during curing and the viscosity of the blend were analysed by rheology studies. A favorable complex viscosity lower than 0.1 Pa*s could be obtained in the pure NCE after heated to 120 ℃, while blending with the EP can dilute and further reduce the viscosity of the monomers to as low as 0.01 Pa*s level. The gel behavior of the copolymers correlates well with the curing thermogram. The viscosity of the mixture gradually increases upon heating and a dramatic rise was found at near the gel point. This gel point was approximately 10 ℃ higher than the curing exotherm onset in these copolymer blends.

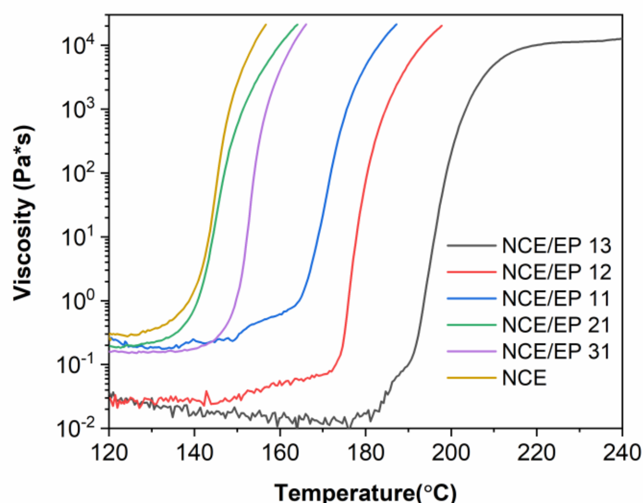

Figure 2.4.3 Viscosity of the uncured NCE and the NCE/EP blends during temperature ramp.

The chemical structures of the cured polymers were investigated by the FTIR seen in Figure 2.4.4. A clear trend of increasing triazine (1543 cm^{-1} and 1360 cm^{-1}) content was evidenced when increasing the NCE feed ratio in the blend, while the copolymerization product oxazolidinone (1743 cm^{-1}) content decreased. It is also worthy to notice that after the curing at 250 ºC for 3 hours, the NCE was not fully cured with evidence of remaining cyanate groups doublet peaks at 2250 cm^{-1}. At the same time, the carbonyl groups were present at ~ 1690 cm^{-1} which could represent the carbamate formation during cure. With adding the EP in the system, conversions of the cyanate groups were more complete. This could be related to the reaction between epoxide and the cyanate groups at the diffusion-controlled stage of curing after gel point, which is kinetically more preferable than the complete conversion of cyanate to form triazine where three cyanate groups need to be brought together.

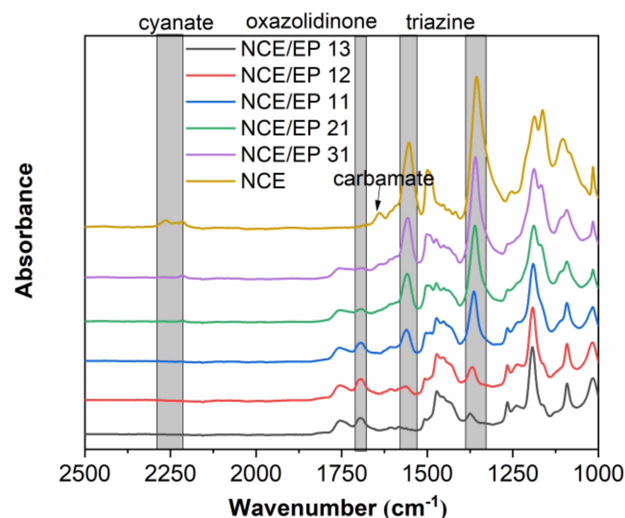

Figure 2.4.4 Chemical structures of NCE and the NCE/ EP blends.

The thermomechanical properties of the NCE/ EP blends were investigated. The parameters from TMA tests are listed in Table 2.4-1. The Tg of the copolymer increased linearly with enlarging the NCE portion in the feed, ranging from 161.04 ºC to 272.51 ºC when the ratio increased from 1:3 to 3:1 ratio. Despite the α_1 all at same level, a large discrepancy was seen in α_2 of the copolymers with different composition. A general trend of first decrease and then increase can be concluded with NCE ratio increased from 1:3 to 3:1, which implied a first increase and then decrease of crosslink density in this series of copolymers.

Table 2.4-1 Parameters from TMA tests on NCE/ EP blends including the T_g and CTE before and after glass transition.

NCE/ EP	TMA T_g/ ºC	α_1/ ppm/ ºC	α_2/ ppm/ ºC

13	161.04	65.42	528
12	220.46	69.25	238.7
11	226.64	75.15	355.2
21	251.04	52.8	133.5
31	272.51	50.87	193.9

Figure 2.4.5 shows the DMA tan δ peaks of these polymers. The parameters extracted from the DMA test including the T_g and rubbery storage modulus used to calculate crosslink density were listed in Table 2.4-2. An extremely high T_g over 400 ℃ was obtained for the pure NCE polymer, which is benefited from the high crosslink density and the stable triazine structure formed by trimerization. Similar to the TMA results, the DMA T_g of the NCE/ EP copolymer showed an increasing trend when increasing the NCE content in the system, which was explained by the more dominate thermally stable and rigid triazine structures presenting in the copolymer. Over 300 ℃ DMA T_g was successfully obtained in the blend system. The damping properties of these sample can also correlate with the crosslink density change when altering the feed ratio of monomers. A first increase and then decease crosslink density was evidenced when increasing NCE/ EP ratio, where the highest crosslink density appears at a moderate NCE concentration. Further increase of the NCE content may cause difficulty in full conversion and decrease the crosslink density. This phenomenon is also in accordance with the trend of α_2 change obtained from the TMA results.

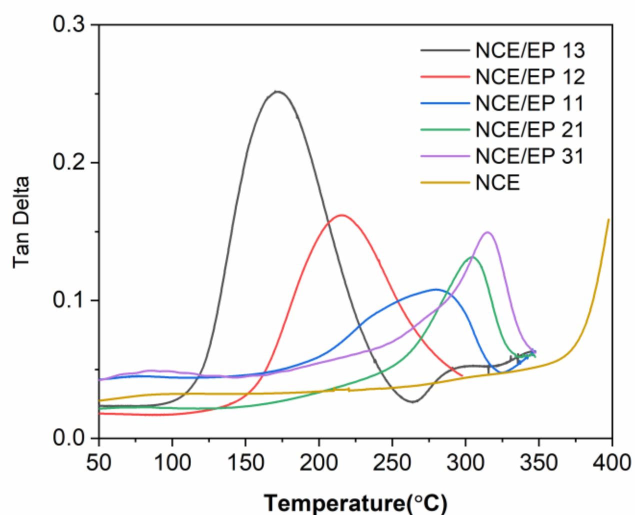

Figure 2.4.5 DMA tan δ profiles of NCE and the NCE/ EP blends.

Table 2.4-2 DMA thermomechanical properties of the NCE/ EP blends, including T_g, storage moduli at rubbery region and the calculated crosslink density.

NCE/ EP	DMA T_g/ ºC	G' at 30 ºC above T_g / Mpa	Crosslink density/ 10^{-3} mol/ cm^3
13	170.14	81.57	16.340
12	214.18	224.8	36.911
11	278.04	170.6	22.204
21	305.81	141.3	16.870
31	314.82	114.3	13.290

The thermal decomposition behavior of these copolymers in N_2 is monitored by TGA tests seen in Figure 2.4.6 and the parameters are summarized in Table 2.4-3. A clear trend of better heat resistance in higher NCE concentrations could be found regarding the decomposition onset (over 400 ºC). The stable triazine structure was credible for the enhancement of thermally robustness of the copolymer network. The high char yield of the polymers (over 60 wt.% remaining at 800 ºC for NCE) could be beneficial for the flame retardance properties.

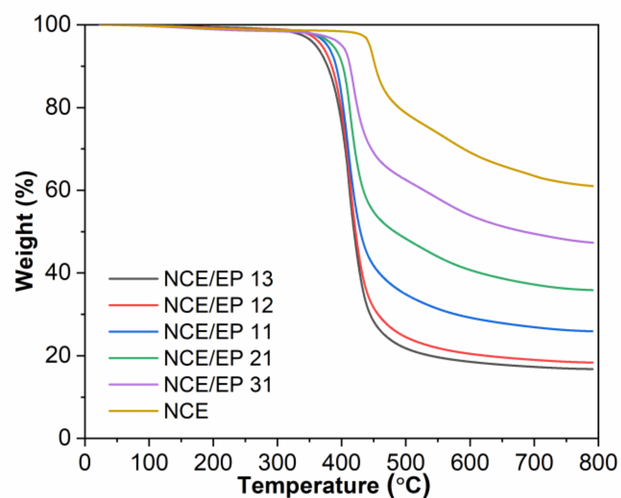

Figure 2.4.6 TGA thermogram of NCE and the NCE/ EP blends in N_2.

Table 2.4-3 Summarized parameters from TGA thermogram of the NCE/ EP blends, including the temperature at 5% and 10% weight loss and residue weight at 800 ℃.

NCE/ EP	$T_{5\%}$ in N_2 / ℃	$T_{10\%}$ in N_2 / ℃	Char Yield at 800 ℃ / %
13	360.19	378.12	16.77
12	269.32	384.65	18.35
11	378.03	391.47	25.91
21	386.47	402.01	35.86
31	400.9	412.99	47.33

10	443.9	452.51	61.02

The moisture absorption behavior of the copolymers under 85 ºC/85 RH condition is graphed in Figure 2.4.7. Higher moisture ingression rate and equilibrium water content was found in higher NCE concentrations, which could be due to the higher polarity of the unreacted cyanate groups within the system [77]. This is also supported by the high D_k of the high NCE content polymers seen in Table 2.4-4. Note that the high EP concentration in the copolymer also caused a high D_k due to the presence of hydroxyl groups, however in this case the methyl groups at the *ortho* position caused steric hindrance and overall suppressed the high moisture absorption in the system.

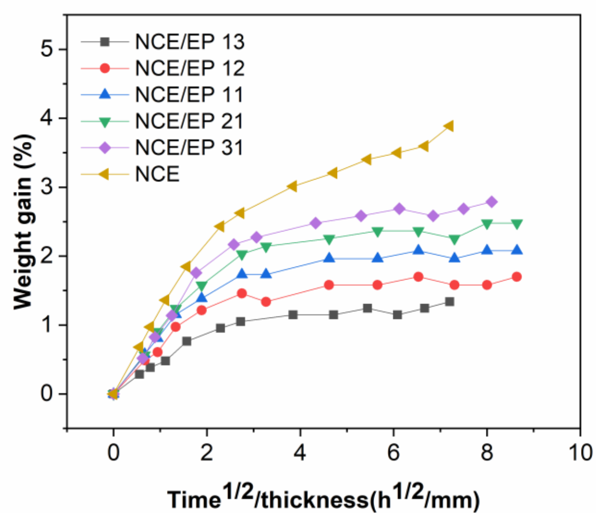

Figure 2.4.7 Moisture absorption of NCE and the NCE/ EP blends under 85 ºC/85 RH condition.

Table 2.4-4 Dielectric constant and loss factor of NCE and the NCE/ EP blends at 10 MHz.

NCE/EP	D_k @ 10 MHz	D_f @ 10 MHz
13	3.68	0.076
12	3.31	0.073
11	3.07	0.069
21	3.23	0.045
31	3.3	0.051

10	3.37	0.031

The high temperature aging performance is important to guarantee the reliability of the EMC under operation. The aging weight loss of the copolymers are depicted in Figure 2.4.8, and the pictures of these samples shown in Figure 2.4.9. The pure NCE exhibited superior heat resistance over the NCE/ EP blends during the first 700 hours. During this period, oxidation may have occurred since the color of the cures resin turned black from orange and sample showed slight shrinkage and blistering. However, further exposure to 250 ℃ caused fast degradation of the pure NCE resin, showing increased weight loss gradients over time and the swollen behavior. During this period, it can still be concluded that the main degradation mechanism should be the outgas produced by the decomposition of carbamate groups in the unreacted cyanate region. Due to the high crosslink density and the extremely high T_g of the resin, this reaction is kinetically suppressed at storage temperature much lower than T_g. However, the high rate absorption of water softening the network structure that lead to the decrease in T_g facilitate the degradation reactions over time. The NCE/ EP blends on the other hand all shared similar characteristics. A first large weight loss can be evidenced before 250 hours, after which the weight loss rate was greatly suppressed. Also, the blistering on sample surface can be noticed and severe volume shrinkage are presented for low CE polymers which indicates the coupling of chain end radicals in the polymer. The degradation behavior is controlled by the trade-off between the oxidation chain scission commonly seen in EP and the carbamate formation due to hydrolysis and its decomposition in the CE part.

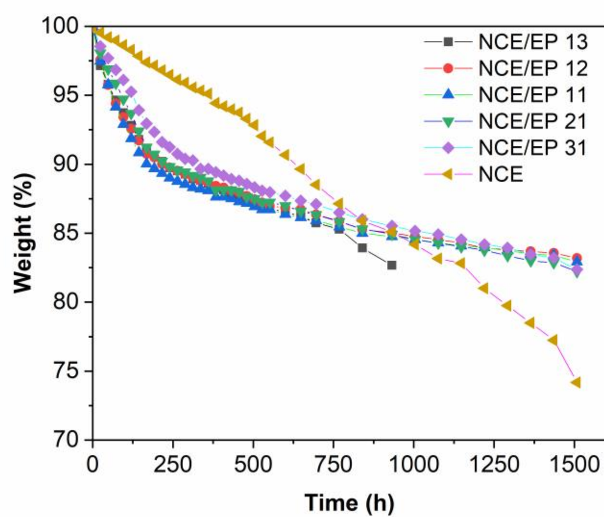

Figure 2.4.8 Weight loss under 250 ºC aging of NCE and the NCE/ EP blends.

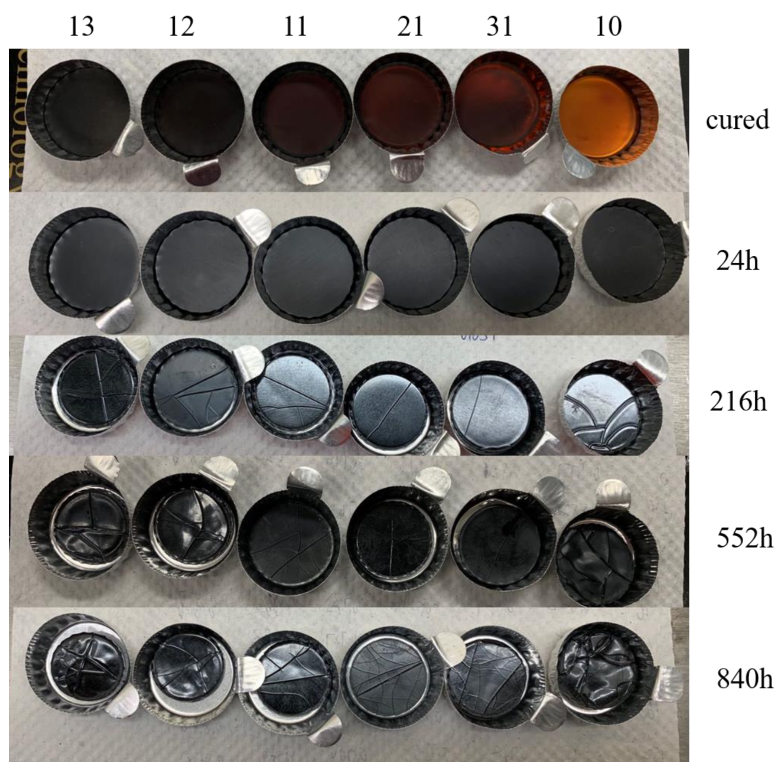

Figure 2.4.9 Picture of the NCE and the NCE/ EP blends under 250 ºC aging, the number above the picture denotes the formulation of the copolymers.

2.5 Conclusion

In this chapter, different approaches have been pursued to enhance the high temperature performance of the previously studied CE/ biphenyl EP blend. The inferior high temperature aging characteristics in the high CE ratio blends was demonstrated, despite their higher T_g and decomposition onset in N_2 seen in TGA, which is mainly attributed to the hydrolysis degradation overtime happen at the region of remaining cyanate groups.

The effects of different metal catalyst on the CE properties were discussed in the first section. The candidates include two types of active metal ions and two types of chelate ligands i.e. Al(III) acac, Cu(II) acac and Cu(II)bzac. It can be concluded that the effect of active metal ion was more dominant than the ligand structure on curing profile as well as the thermal aging properties. The Cu^{2+} ions were more efficient in facilitating the trimerization of CE, showing decreased curing temperature compared to Al^{3+} ions as well as a wider exothermic peak. Moreover, the lower tendency of forming carbamate in the Cu^{2+} catalysed CE resulted in a prolonged storage life under high temperature, compared to the early fail using Al^{3+} catalyst. In the CE/EP blends (1:1), two separate curing exotherms were evidenced in the Cu^{2+} catalysed polymers. These two peaks were determined by FTIR, where the low temperature peak represents the trimerization of CE molecules to generate triazine and crosslink, and the high temperature one the copolymerization of epoxide and formed triazine structure.

To exploit the benefits of triazine structure on increasing T_g and short-term heat resistant while alleviate the hydrolysis problem from unreacted CE, a triazine containing

molecule TGIC was employed as an epoxy source to directly insert the triazine structure and their thermomechanical properties were characterized in the second section in this chapter. Thanks to the trifunctional (which can result in higher crosslink density in the cured resin) and aromatic nature, the addition of TGIC effectively increased the T_g of CE/EP blend at low loading. Further increasing the TGIC content led to a competition between increasing crosslink density and the plasticizing effects of unreacted small molecules and may reduce the T_g. The thermal decomposition behavior were improved at the same time. However, due to the high moisture absorption rate in the TGIC incorporated polymers, a large weight loss during high temperature aging was observed.

The high heat resistant novolac type CE was employed to form the NCE/EP blend, and the blends with different feed ratio were systematically evaluated in the third section in this chapter. The very high T_g over 400 ºC from DMA was observed in the pure NCE, and the increase of NCE content in the NCE/EP blend significantly increased the T_g as well as decomposition onset of the polymer. The EP on the other hand was found to dilute the viscos NCE and reduce the viscosity to render processability. The pure NCE exhibited superior heat resistance under 250 ºC aging condition than the NCE/EP blends in the first 700 hours while a large weight loss gradient and swelling was observed in further aging. The extremely high T_g prolonged the lifetime at relative low aging temperature. However, the high moisture absorption plasticized the network and facilitated the hydrolysis degradation and eventually the failing pattern was similar to the bisphenol A CE. All other blends on the other hand showed a suppressed weight loss profile after the initial drop, and the effect of composition of the copolymer was not evident. The mid NCE content

compositions have great potential for future high temperature molding applications with these intriguing features.

CHAPTER 3. DEVELOPMENT AND FAILURE ANALYSIS OF NOVOLAC EPOXY/TRIAZINE BASED HIGH TEMPERATURE STABLE RESIN SYSTEMS

To further enhance the high temperature performance of the cyanate ester (CE)/ epoxy (EP) blend, novolac type EP including epoxy phenol novolac (EPN) and epoxy cresol novolac (ECN) were adopted in the system. This chapter presents the works on evaluating a CE/ECN blend resin system regarding their thermomechanical properties and other properties important to the molding application. Moreover, the aging degradation on the polymer physical and chemical properties is discussed in the last section.

3.1 Materials and Experimental

DEN 431 resin (EPN1) were obtained from Dow Chemical with a E.E.W. of 177. EPON 160 resin (denoted as EPN2) were supplied by Hexion Inc., with a E.E.W. of 173. ESCN 195XL resin (ECN) was obtained from Sumitomo Chemical, with a E.E.W. of 195. Bisphenol A cyanate ester was purchased from Oakwood Chemical. Copper (II) acetylacetonate and nonylphenol were purchased from Aldrich and used as received.

Due to the large melt viscosity, solvents will be used to achieve good mixing of the monomers. Acetone is used for dissolving the CE monomer assisted by sonication. The well mixed solution was later placed in vacuum oven to remove all the solvents before curing. The CE/ECN blend formulations were calculated based on functional group molar ratios. In the screen test, all epoxide to cyanate ratios were kept at 1:1. The Cu^{2+} catalyst was loaded at 360 ppm and the nonylphenol at 3 phr to the CE weight.

Differential Scanning Calorimetry (DSC) was done by DSC Q2000 from TA Instrument to characterize the curing thermo profile of the polymer mix. The experiments were ramping at 10 ℃/min and were done under nitrogen atmosphere. Thermal Mechanical Analysis (TMA) was done using TMA Q400 from TA Instrument. Ramping rate was kept at 20 ℃/min and experiments were under nitrogen atmosphere. Dynamic Mechanical Analysis (DMA) was performed by DMA Q800 from TA Instrument in tension mode. Ramping rate was 3 ℃/min at oscillation frequency 1 Hz. The Thermal Gravimetric Analysis (TGA) both under nitrogen and air atmosphere used TGA Q5000 from TA Instrument. All tests programmed to ramp 20 ℃/ min to 800 ℃. Dielectric properties of the sample were tested by Agilent E4991A RF Impedance Analyzer. Fourier-transform Infrared spectroscopy (FTIR) was done by Thermo Scientific Nicolet iS5 FT-IR spectrometer using a diamond ATR mode. The high temperature aging test was done in the Fisher Scientific 825f convection oven and the moisture absorption done in MicroClimate bench top environmental chamber from Cincinnati SubZero Inc.

3.2 Screen Test on Novolac Type Epoxy/Triazine Copolymers

The structure of the novolac type EP is shown in Figure 3.2.1. They are normally synthesized by epoxidizing the reaction product of phenol-formaldehyde (for EPN) or that of cresol-formaldehyde (for ECN). The novolac epoxies are known to support higher crosslink density due to their high functionality per molecule [78, 79], which can lead to the increase of T_g and enhancement of heat resistance. In the CE/EP system, it is thus inferred that the copolymer between CE and novolac EP are beneficial for the high

temperature stability. In the following section, the thermal mechanical properties of different types of CE/ ECN or CE/ EPN blends are summarized. The best performance copolymer is then discussed in more details regarding the effects of the resin formulation on its properties and the high temperature aging degradation mechanism.

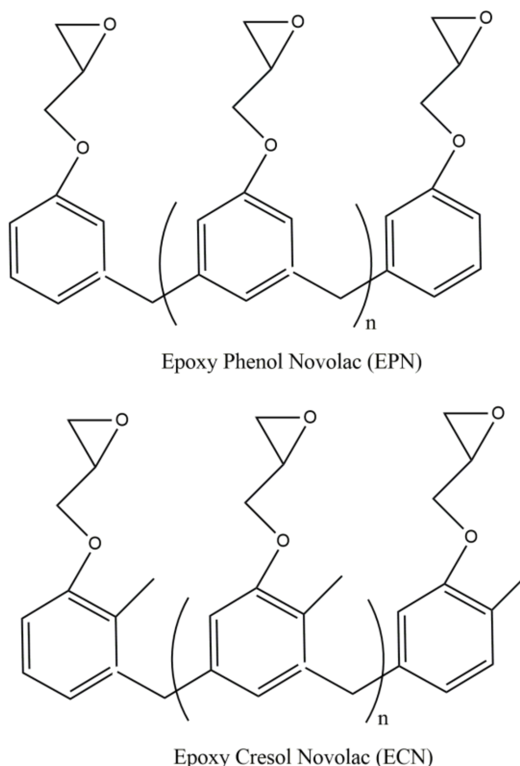

Figure 3.2.1 Chemical structure of typical epoxy phenol novolac (EPN) and epoxy cresol novolac (ECN).

A quick screen test on different types of EPN or ECN when blending with CE was done first regarding their thermal decomposition behaviour and high temperature storage weight loss. Two types of EPN and one type of ECN were selected as candidate for this purpose. A a screen test, all epoxide to cyanate groups molar ration was kept at 1:1. The Figure 3.2.2 showed the N_2 purged TGA profile of these copolymers in comparison with

the previously used CE/ biphenyl type EP copolymer. From the magnified region, a clearly higher decomposition onset could be found for the CE/ EPN and CE/ ECN blends. This is mainly attributed to the high crosslink density within the resin and the large stable segments between the weak ether bonds originated from the novolac structure. At the same time, a significantly higher char yield after the decomposition in the CE/ EPN and CE/ ECN blends denotes the larger char forming tendency of these polymers which is in accordance with their closely crosslinked structures. The high char residues can generally enhance the flame retardancy of the thermoset materials since they can increase difficulty of oxygen diffusion and prevent further combustion.

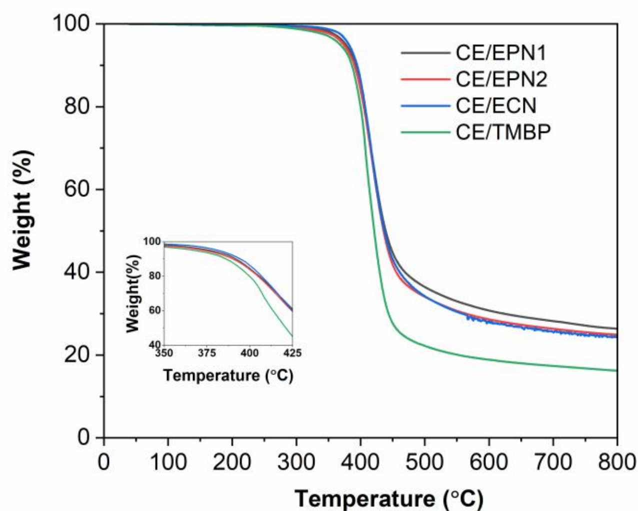

Figure 3.2.2 TGA thermogram of the copolymer between CE and two types of EPN, one ECN and the previously used TMBP. The inset magnifies the 350 ºC~ 425 ºC region.

The long-term heat resistance of these copolymers is presented in Figure 3.2.3. Unlike the behaviour in TGA ramp, the two copolymer consist of EPN type EP exhibited

inferior integrity compared to that consists of biphenyl EP. On the other hand, the CE/ECN copolymer showed similar weight loss behavior compared to the CE/TMBP blend. Moreover, the TMA T_g of the CE/ECN is over 30 ℃ higher than the CE/TMBP (Table 3.2-1). Considering the overall performance, CE/ECN is determined to be the choice as high-performance EMC resin material. In the following contents, the effects of CE to ECN ratio of the materials properties were systematically evaluated.

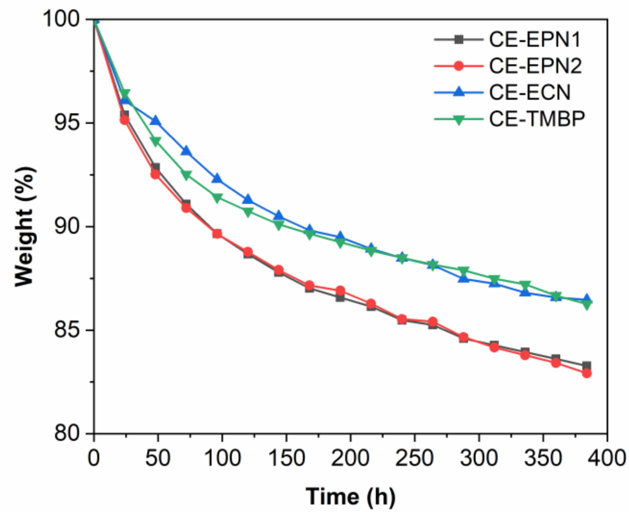

Figure 3.2.3 Weight loss under 250 ℃ aging of the copolymer between CE and two types of EPN, one ECN and the previously used TMBP.

Table 3.2-1 Comparison of TMA T_g of CE/TMBP blend and CE/ECN blend. (epoxide: cyanate molar ratio at 1:1)

Sample	TMA T_g/ ℃
CE/TMBP	218.54

CE/ECN	235.84

3.3 Evaluation on Epoxy Cresol Novolac/Triazine Resin System

The curing profile of the CE/ECN at different feed ratio is shown in Figure 3.3.1. Compared to the previously studied biphenyl EP and CE blend, the exothermic peaks were more complicated in this case. However, the CE/EP curing characteristics and trends with concentration increments could still be found in these copolymer systems. For example, in the 1:1 ratio system, there are two major peaks evidenced with onset at roughly 125 ºC and 225 ºC, respectively, which is similar to the CE/TMBP case. Moreover, the area under the first exothermic peak increased with increasing CE concentration and the second decreased. It was also noted that the high EP ratio copolymers experienced less exothermic heat during the curing reaction.

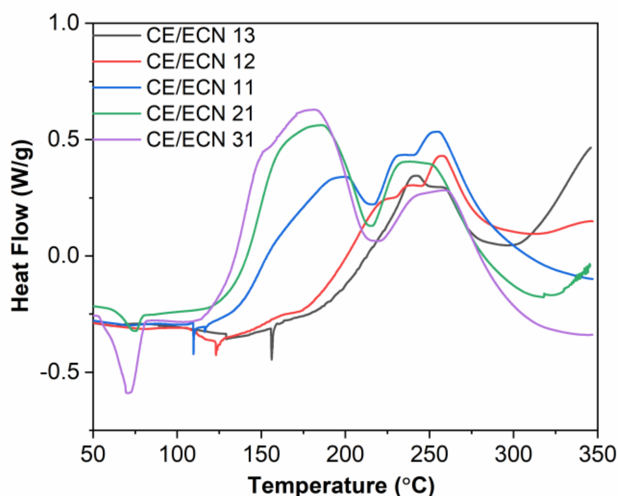

Figure 3.3.1 DSC curing thermogram of the CE/ECN blends at different ratio , ranging from 1:3 to 3:1 on molar ratio between cyanate groups and epoxide groups.

It was suspected that the origin of these two peaks are similar to the CE/TMBP system, which is supported by the in situ FTIR with same ramping rate as the dynamic DSC scan (Figure 3.3.3). Still, when heating over the first exotherm, the consumption of cyanate groups (2250 cm^{-1}) and appearance of triazine rings (1360 cm^{-1} and 1543 cm^{-1}) indicates the trimerization reaction of CE part, while no change of epoxide groups (915 cm^{-1}) was noticed during this period. In the temperature range over 200 ºC, the epoxide intensity was decreasing and the oxazolidinone carbonyl groups (1747 cm^{-1}) were emerging. At the same time, the triazine groups intensity decreased which is in accordance with the reaction route involving the insertion of epoxide on triazine and rearrangement to oxazolidinone.

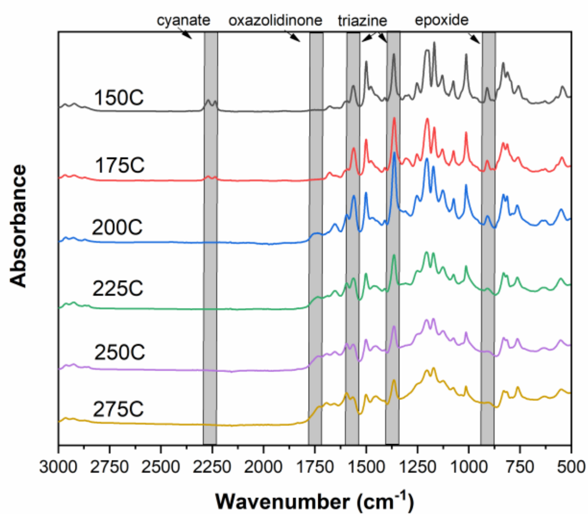

Figure 3.3.2 FTIR spectra of CE/ECN blends at 1: 1 molar ratio during temperature ramp.

The chemical structure of the CE/ECN blends with different feed ratio is shown in Figure 3.3.3. It can be concluded that with increasing CE components in the system, higher triazine intensities appeared. At the same time, the observance of oxazolidinone groups required high ECN contents in the system.

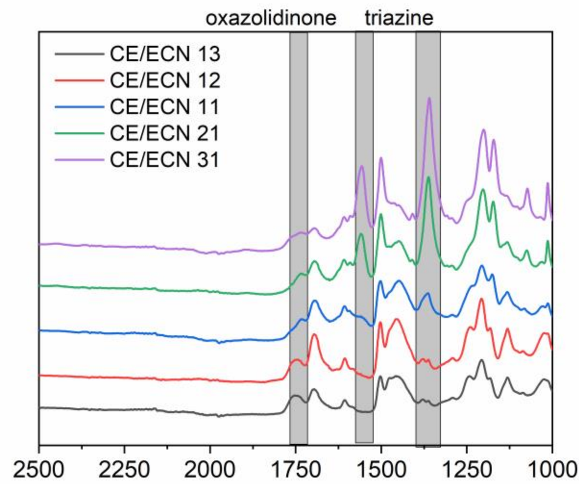

Figure 3.3.3 FTIR spectra of CE/ECN blends with different feed ratio.

Thermomechanical properties of the cured CE/ECN blends were investigated by TMA and DMA tests. The Table 3.3-1 summarized the parameters from the TMA study. An increasing TMA T_g was shown when the ratio between cyanate groups to epoxide groups rise from 1:3 to 3:1. The 3:1 blend achieved a high T_g of near 250 ºC. Also, considering the rubbery stage CTE, an initial decrease and then increase during increasing CE content indicated an opposite trend of crosslink density of the polymer.

Table 3.3-1 Parameters from TMA tests on CE/ECN blends including the T_g and CTE before and after glass transition.

CE/ ECN	TMA T_g/ ºC	α_1/ ppm/ ºC	α_2/ ppm/ ºC
13	203.52	67.21	228.7
12	221.99	64.61	216.7

11	235.84	60.95	160.1
21	237.85	58.3	253.8
31	248.91	60.37	279.7

The DMA tan δ profiles on the CE/ECN blends from 1:3 to 3:1 molar ratio are presented in Figure 3.3.4. The DMA T_g of the copolymer increased from 221.07 ºC to 247.58 ºC when increasing CE concentration from 1/3 to 1/2 ratio in the system. However, further enlarging the CE feed ratio did not lead to obvious increase in the T_g of the copolymer. Furthermore, the damping property were found to increase at the same time. A more detailed look of the polymers ranging from 1/3 to 1/2 ratio are shown in Figure 3.3.5. A continuous incremental T_g can be evidenced when pushing the CE content in this range with shrinking damping properties. The explanation for these phenomena was explained by the competition between the triazine structure content in the system and the crosslink density of the copolymer. The properties calculated based on DMA data are listed in Table 3.3-2. In the relative low CE content copolymers, raising CE feed ratios concurrently increased the content of the rigid triazine structure and the crosslink density (due to higher conversion of epoxides to oxazolidinone), and thus promoted the T_g growth. However, at the high CE content region, due to the lack of high functionality ECN monomers, the crosslink density of the resin would rather decrease upon increasing CE parts. This trend is also supported by the previously mentioned α_2 measured by TMA. The balanced off the effects of growing triazine structures contents in the resin during this CE feed increase, and

thus caused the T_g increase to be negligible. The evidenced first decreased and then increased damping factors matched well with the first increased and then decreased crosslink densities of these polymer when raising CE ratio. The low crosslink density samples exhibited larger tendency of dissipating applied energy.

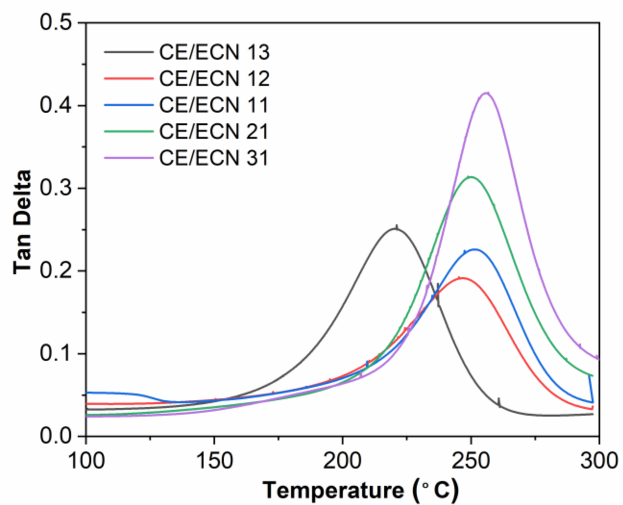

Figure 3.3.4 DMA tan δ profiles of CE/ECN blends ranging from 1:3 to 3:1 on molar ratio.

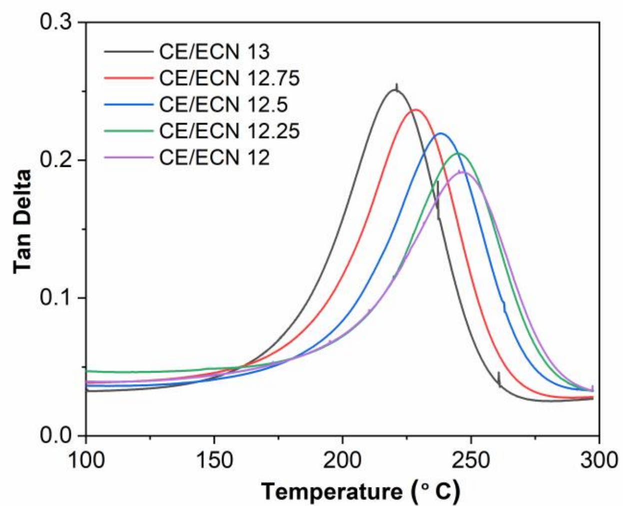

Figure 3.3.5 DMA tan δ profiles of CE/ECN blends ranging from 1:3 to 1:2 on molar ratio.

Table 3.3-2 DMA thermomechanical properties of the CE/ECN blends, including T_g, storage moduli at rubbery region and the calculated crosslink density.

CE/ ECN	DMA T_g/ ºC	G' at 30 ºC above T_g / Mpa	Crosslink density/ 10^{-3} mol/ cm^3
13	221.07	114.5	18.284
1 2.75	228.6	129.8	20.124
1 2.5	238.52	134	20.008
1 2.25	245.25	154	22.432
12	247.58	133.1	19.225
11	251.73	130.5	18.571
21	248.87	115.7	16.634
31	256.74	61.34	8.577

The thermal decomposition profile of the CE/ECN blends in N_2 are given in Figure 3.3.6, and the weight loss derivative over temperature in Figure 3.3.7. The parameters extracted from the TGA and DTG analysis are summarized in Table 3.3-3. From this magnified region in TGA and the DTG profile, low CE content polymers exhibited a lower decomposition onset compared to the high CE content polymers. However, these low CE resins exhibited better heat resistance after the first 10 wt.% of decomposition, showing higher temperature at peak decomposition rate (T_p). When increasing CE concentration at

feed, the decomposition onset was pushed towards higher temperature, while a large weight loss gradient was observed right after the initial decomposition and accordingly the T_p was decreased. This phenomenon can be explained by the competition between increasing triazine contents in the network and the decreasing crosslink density and the number of large aromatic molecules between ether linkages when increasing CE concentration in the feed material. Although less triazine nodes were formed in low CE content polymers and the the onset temperature of decomposition were found to decrease, the weight loss after the initial stage was more kinetically controlled by the over network structure which is suppressed here due to the high crosslink density in the system. Moreover, the main building blocks of these resin are large and highly aromatic molecules between the weak ether linkages. After the onset of decomposition, these large molecules are less likely to be broken or evaporated. These features contributed to the unique behavior of the CE/ECN system on the resisting the heat.

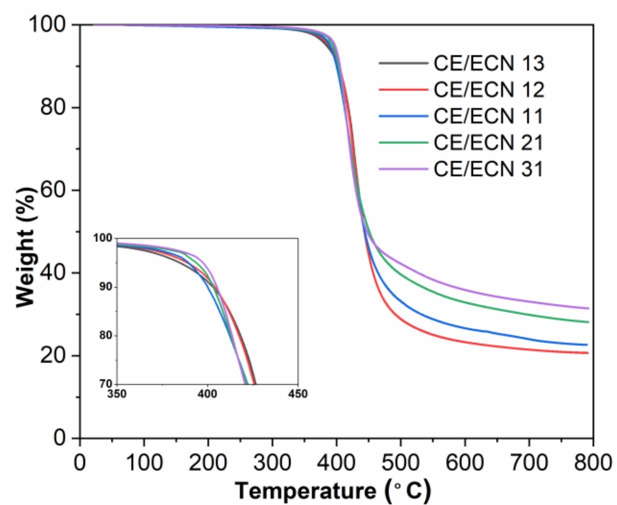

Figure 3.3.6 TGA thermogram of CE/ECN blends in N_2. The inset magnifies the 350 ºC~ 450 ºC region.

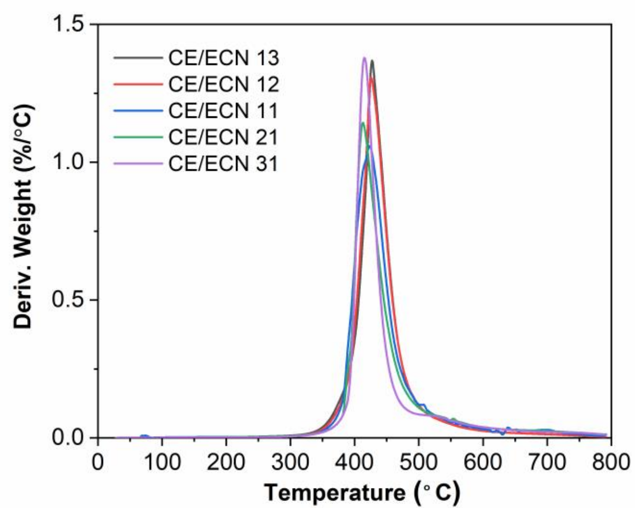

Figure 3.3.7 DTG thermogram of CE/ECN blends in N_2.

Table 3.3-3 Summarized parameters from TGA and DTG thermogram of the CE/ECN blends, including the temperature at 5% and 10% weight loss, residue weight at 800 ºC, initial decomposition temperature and peak decomposition temperature.

CE/ ECN	$T_{5\%}$ in N_2 / ºC	$T_{10\%}$ in N_2 / ºC	Char Yield at 800 ºC / %	T_i / ºC	T_p / ºC
13	384.7	403.12	20.7	393.16	427.22
12	388.95	404.11	20.65	390.38	425.75
11	389.5	400.18	22.62	381.14	423
21	393.82	403.21	28.13	390.19	412.91
31	397.49	405.2	31.45	392.22	415.17

The moisture absorption behavior of the polymers blends when subjected to 85 ºC/ 85 RH condition is graphed in Figure 3.3.8. Similar to the case of previously studied CE/EP system, the CE still possessed the highest moisture ingression rate and the equilibrium water containment. The mixing with ECN caused decreased moisture absorption, however the trend when comparing different compositions were not distinguishable. Roughly the lower CE content polymers showed reduced water uptake, which is possibly be due to the high crosslink density seen in these resins. It is interesting to find that the dielectric constant of the copolymer actually decreased when increasing the CE feed ratios, as can be noticed from Table 3.3-4. This indicated the decrease of polarity in these polymers due to the lack of EP components and therefore the polar hydroxyl groups.

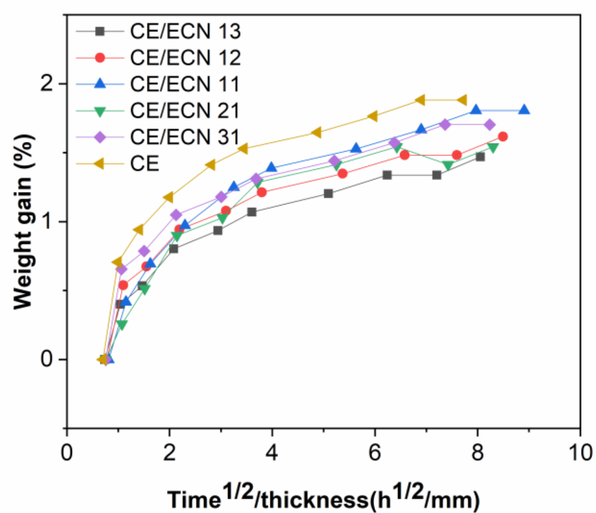

Figure 3.3.8 Moisture absorption of CE/ECN blends under 85 ºC/85 RH condition.

Table 3.3-4 Dielectric constant and loss factor of CE/ECN blends at 10 MHz.

CE/ ECN	D_k @ 10 MHz	D_f @ 10 MHz
13	3.25	0.023
12	3.33	0.02
11	3.11	0.022
21	3.08	0.026
31	2.95	0.017

3.4 High Temperature Aging Effects on Epoxy Cresol Novolac/Triazine Copolymers

Figure 3.4.1 shows the high temperature storage test results on the CE/ECN blends. Although the pure CE exhibited preferred thermal stability in the initial 3~4 days, a large weight loss gradient was associated with the swelling and blistering of the sample that lead to early fail within 10 days. On the other hand, all the CE/ECN blends experienced a large initial decomposition which is followed by the slow weight loss over time. Also, it is worth noticing that similar to the CE/EP blend studied by our group before, high CE content copolymers generally presented larger weight loss tendency during the high temperature aging, especially after the initiation of drastic weight drop in pure CE. For the 3:1 CE/ECN sample, 1500 hours of aging led to a residue of the sample less than the char yield in TGA test in N_2, indicating the strong oxidation reactions during the high temperature storage. The pictures of the sample during the high temperature storage are shown in Figure 3.4.2. Clearly the high CE samples showed early shrinkage and warpage during aging, while the low CE polymers maintained its shape up to 300 hours before the blistering. Knowing the high T_g and high decomposition onset temperatures in the high CE polymers, it is to be further understood why these polymers tend to fail and decompose drastically under aging condition, which is believed to associate with the behavior of the CE parts in the resin.

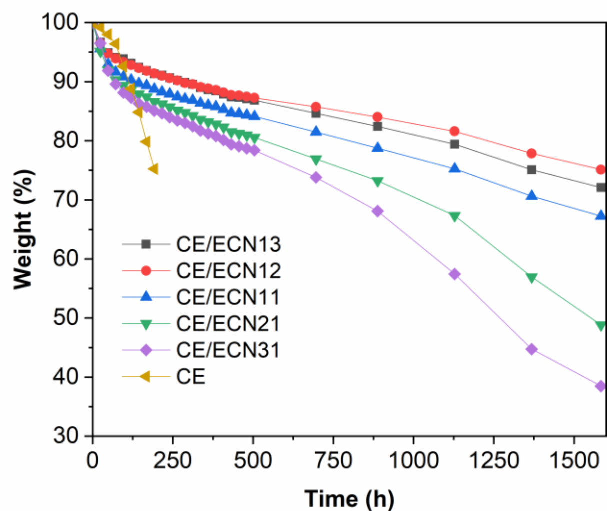

Figure 3.4.1 Weight loss under 250 ºC aging of CE/ ECN blends.

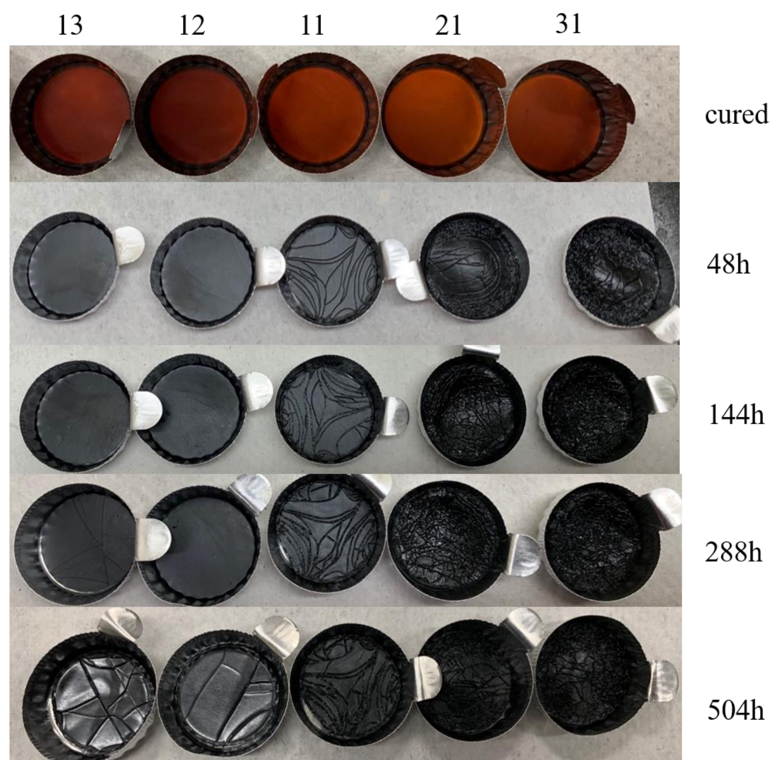

Figure 3.4.2 Pictures of CE/ ECN blends under 250 ºC aging. The number on top of the picture denotes the formulation of the copolymer.

Other than the aging weight loss behavior, the TMA tests were employed to illustrate the effect of high temperature storage on the thermomechanical property of these resins. Table 3.4-1 summarized these property changes during the aging test in the first 48 hours, where the formulation 1:3, 1:1 and 3:1 were selected to represent the materials nature. In the 1:3 sample, a first increase and then decrease T_g could be found during aging, while the change of α_2 was in the opposite trend. It has been known that further curing could take place when an EP sample is exposed to elevated temperature for prolonged time [80]. In this case, it is likely that the EP dominated resin went through curing reaction to build up a higher crosslinked network in the first several hours of aging, as evidenced by the T_g increase and α_2 decrease. However, as the aging temperature is higher than the T_g of the polymer, not only the curing but also degradation which is controlled by oxygen diffusion was facilitated. The breakdown of network took place during longer time of curing, resulting in the decrease in crosslink density and the T_g of the polymer.

Similar to the CE/ECN 1:3 polymer, the 1:1 formulation showed a slightly increased T_g after aging for 4 hours. Continue heating the sample will cause the decrease in T_g and increase in α_2, which is the sign of chain scission and network breakdown due to oxidative degradation. However, the 3:1 polymer exhibited different behavior than the low CE content resins. Although the virgin 3:1 sample processed the highest T_g among all the formulations, the dramatic and continuous T_g decrease was evidenced in the sample. At the same time, the variation of α_2 was not obvious. This implies that the crosslink density change due to chain scission may not be appreciable during aging in this polymer. Considering the high moisture absorption in this polymer and the sensitivity of CE to

hydrolysis, this behavior could be related to the plasticization effects of absorbed water and the outgas reactions during aging.

Table 3.4-1 Parameters from TMA tests on CE/ECN blends during aging under 250 ºC aging including the T_g and CTE before and after glass transition.

CE/ECN	Aging time/ h	TMA T_g/ ºC	α_1/ ppm/ ºC	α_2/ ppm/ ºC
13	0	203.52	67.21	228.7
	4	237.5	77.69	192.3
	8	226.6	75.66	198
	24	201.42	65.99	247.2
	48	200.56	75.14	489.5
11	0	235.84	60.95	160.1
	4	238.34	79.67	234.4
	8	203.65	65.44	251.3
	24	202.45	71.04	344.5
	48	161.27	65.81	290.1
31	0	248.91	60.37	279.7

4	239.02	59.46	303.5
8	210.47	51.77	295.6
24	189.57	68.47	224.3
48	173.24	97.15	275.7

The chemical structure change of these polymers during aging were monitored by FTIR. The track down on FTIR of CE/ECN 1:3, 1:1 and 3:1 polymer blend upon aging is shown in Figure 3.4.3, Figure 3.4.4 and Figure 3.4.5, respectively. From Figure 3.4.3, one can first notice the disappearance of epoxide absorption peaks at 915 cm^{-1} during aging for 4 hours. This indicates the further curing of the EP rich polymers under elevated temperature far above T_g. As a result, the intensity of C-O stretching peak (broad peak around 1250 cm^{-1}) was observed, as well as the O-H peaks (bending at around 1420 cm^{-1} and stretching at 3200 cm^{-1}) due to formed ether or ester structures. This further curing is also in agreement with the observed TMA T_g increase in the initial aging stage. However, during further exposure to the high temperature, severe oxidative degradation took place. The peak intensity of C=O groups (the one at 1660 cm^{-1} can be attributed to amide and the 1740 cm^{-1} to ketone or aldehyde) as well as that of the C-O and hydroxyl groups grew monotonically over time. It can be inferred that the degradation scheme of high EP content CE/ECN copolymer was dominated by the typical EP thermo-oxidation pattern through the chain scission assisted by radicals reacting with oxygen, causing the decomposition of network structure [23, 28, 29]. Similarly, the CE/ECN 1:1 copolymer exhibited the further consumption of epoxide groups during high temperature storage. However, the increase of

hydroxyl groups are not obvious upon further aging. Still, the growth on C=O and C-O fractions in the polymer indicated the thermo-oxidation taking place. Note that the rapid increase of intensity on C=O amide groups could be also attributed to the formation of carbamate groups from the CE part. In the high CE content polymer, i.e. the CE/ECN 3:1 formulation, degradation mechanism was different from the low CE ones. In Figure 3.4.5, compare to previously discussed formulations, the consumption of epoxide groups or the formation of ether bonds were not observed, despite the longer aged sample showed weakened IR signal due to the roughened surface. Meanwhile, the trend of increasing carbonyl intensity can be clearly identified which could correlate with the growing intensity of amine groups (N-H stretching at 3400 cm^{-1}) that indicated the formation of carbamate groups in the resin. Also, the intensity of triazine groups which were dominant in the cured resin gradually decreased over time. It has been reported that under hydrolysis conditions the attack of water on the weak ether linkages attached to the triazine ring can cause the cleavage of the ring structures at [81]. However, considering that no apparent crosslink density change was observed during the curing (or rather increase), this mechanism may not be applied in this high temperature aging condition. The reformation of triazine to isocyanurate structures may be the main reason of decrease of triazine amount. The decomposition of the observed carbamates here can lead to the outgas and deformation of the physical network, which were the main cause of the large weight loss and T_g decrease in the high CE content polymers. This process can generate stress within the resin and finally lead to failure of the sample.

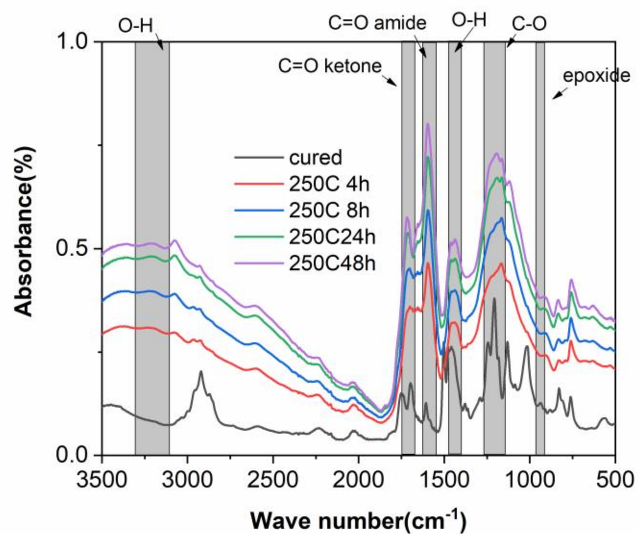

Figure 3.4.3 FTIR spectra of CE/ECN 1:3 blend during 250 ºC aging.

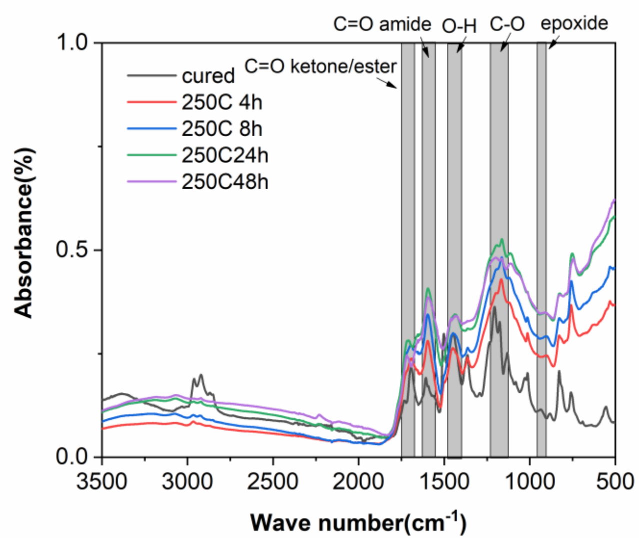

Figure 3.4.4 FTIR spectra of CE/ECN 1:1 blend during 250 ºC aging.

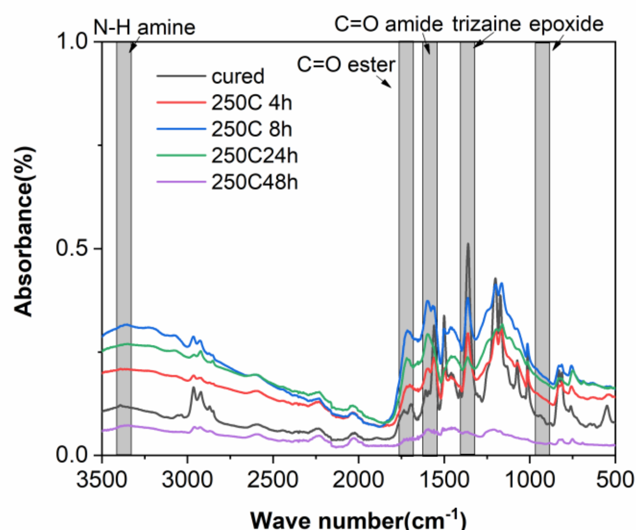

Figure 3.4.5 FTIR spectra of CE/ECN 3:1 blend during 250 ℃ aging.

The thermal decomposition behavior of the aged samples were also characterized. The Figure 3.4.6, Figure 3.4.8 and Figure 3.4.9 shows the aging effects on the TGA tests of CE/ECN 1:3, 1:1 and 3:1 blends, respectively. The parameters from TGA and DTG analysis are summarized in Table 3.4-2. Note that these weight profiles of the aged samples were not normalized according to their initial weight loss due to aging, otherwise the aged sample curves should be shifted down in weight. For all of the formulations, higher residue weight was shown in the high temperature region. This is partially because of the lower initial weight of aged sample compared to virgin sample due to the decomposition happened during high temperature storage. However, if normalize these char yields using the aging weight loss data (as seen in Figure 3.4.1), it could be found that the aged sample still possessed larger char residue (for example in Figure 3.4.7), indicating the further crosslinking they experienced during aging that caused a better char forming ability.

The onset of decomposition is more of interest to infer the chemical and physical changes during high temperature aging. In Figure 3.4.6, an obvious higher decomposition onset was observed after aging conditions. To account for the weight loss already occurred during aging, a normalized weight diagram is given in Figure 3.4.7 according to the weight loss during aging characterized before. A better matching regarding the weight loss profile of the unaged and aged samples was found. It can be inferred that the first stage of the thermal decomposition (the difference between aged and virgin sample) might have already took place. Besides, from the magnified region as well as the T_i data in Table 3.4-2, it is clear that the 48 hours aged sample exhibited better heat resistance than the virgin sample. This could be explained by the further vitrification of resin and the depletion of the most thermally unstable ether bonds [82]. With longer aging time, this effect was diminished as the decomposition of the breakable structure. The side reactions in typical EP would take place during this period including the ring forming reactions to render a better char forming ability.

Unlike the low CE CE/ECN blends, when increasing the feed ratio of CE in the resin, aging would cause a decrease of the onset decomposition temperature. For example, in Figure 3.4.8, the 48 hours aged CE/ECN 1:1 sample showed similar weight loss profile as the virgin sample. If normalizing the curve, the downshift of the weight can reveal the decreased decomposition temperature. The curing effects of EP became less appreciable in the higher CE content polymers. Longer exposure of the sample to high temperature showed clearer trend of the decreased onset temperature, as seen in Table 3.4-2. The 120 hours and the 192 hours aged samples somehow exhibited similar weight loss pattern. Recall from Figure 3.4.1, the aging of sample over roughly 96 hours seen a greatly reduced

the weight loss to rate. The 120 hours and 192 hours aged sample all belong to this category, where the resin achieved a steady decomposition stage due to the lack of easily breakable chemical structures.

The high CE ratio blends exhibited interesting decomposition results after aging. In Figure 3.4.9, a much inferior thermal stability was found for the 48 hours aged samples. As previously mentioned, the CE/ECN 3:1 ratio copolymer experienced linear T_g decrease during curing, while the crosslink density change was negligible. Moreover, the FTIR revealed the main degradation mechanism was based on the carbamate formation reactions through hydrolysis. It is inferred that the instability of the resin was not due to the chemical structure changes in the resin (oxidative degradations), but rather the induced mechanical stress resulted from the outgas. Longer aging on the other hand showed a similar onset decomposition temperature as the virgin sample, while possessing much higher char yields. The thermal stress within the sample might have been relieved through rearrangement and the decomposition was less violent. High char forming ability could be benefited from the further reaction between the amine from carbamate and the epoxide groups in the resin.

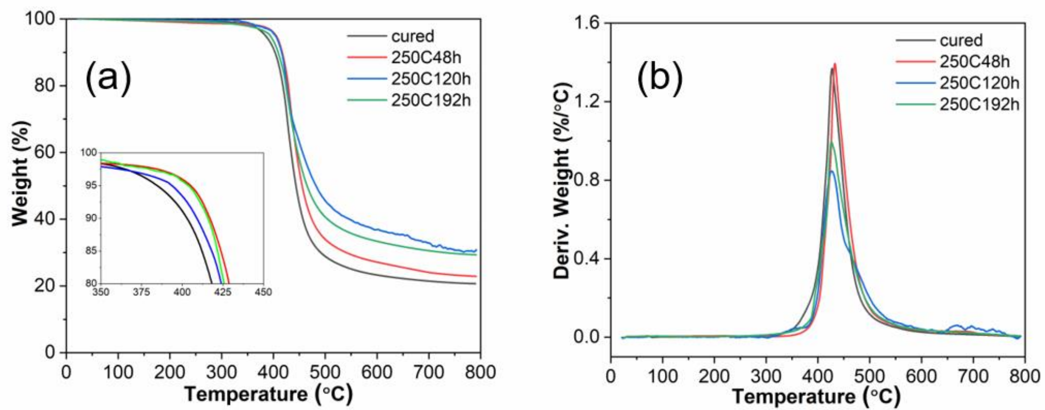

Figure 3.4.6 (a) TGA and (b)DTG thermogram of CE/ECN 1:3 blends after aging in 250 ºC for different time in N_2. The inset in (a) magnifies the 350 ºC~ 450 ºC region.

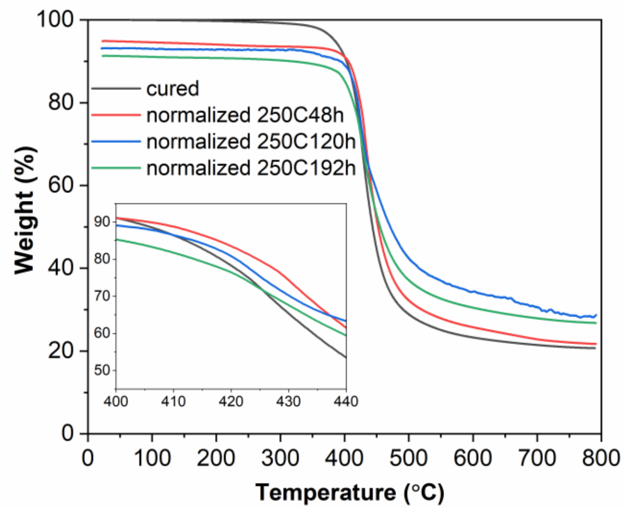

Figure 3.4.7 Normalized TGA thermogram of CE/ECN 1:3 blends after aging in 250 ºC for different time in N_2. The inset magnifies the 400 ºC~ 440 ºC region.

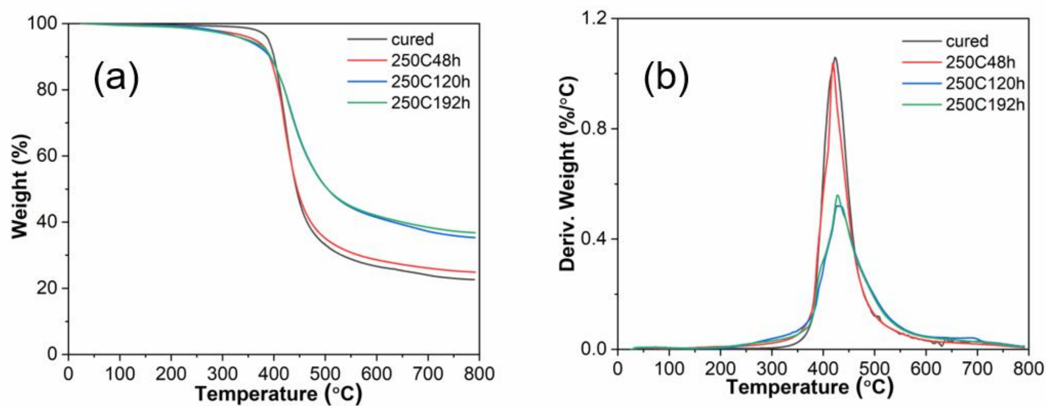

Figure 3.4.8 (a) TGA and (b)DTG thermogram of CE/ECN 1:1 blends after aging in 250 ºC for different time in N_2.

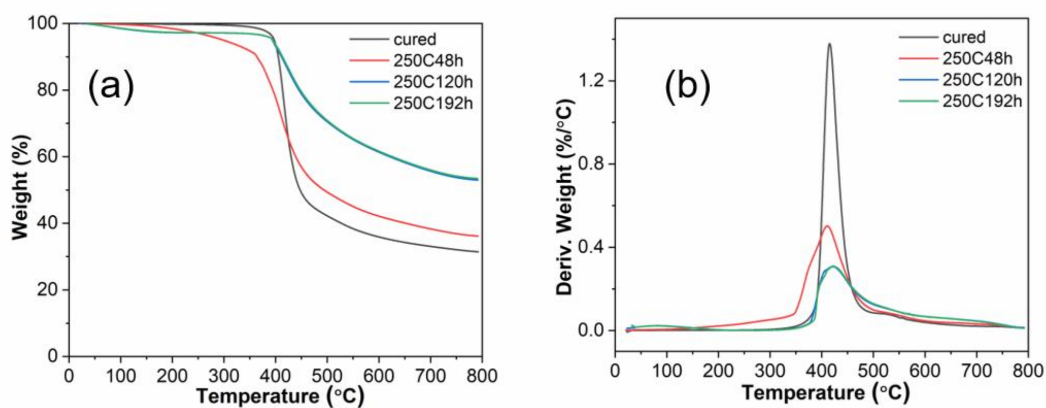

Figure 3.4.9 (a) TGA and (b)DTG thermogram of CE/ECN 3:1 blends after aging in 250 ºC for different time in N_2.

Table 3.4-2 Summarized parameters from TGA and DTG thermogram of the CE/ECN blends after aging under 250 ºC for different time, including the temperature at

5% and 10% weight loss, residue weight at 800 ºC, initial decomposition temperature and peak decomposition temperature .

CE/ECN	Aging time/ h	$T_{5\%}$ in N_2 / ºC	$T_{10\%}$ in N_2 / ºC	Char Yield at 800 ºC / %	T_i / ºC	T_p / ºC
13	Cured	384.7	403.12	20.7	379.78	423
	48	405.28	417.09	22.9	377.03	418.81
	120	403.54	415.85	30.57	377.96	427.98
	192	393.78	409.1	29.35	377.39	427.92
11	Cured	389.5	400.18	22.62	391.96	427.22
	48	364.26	391.7	24.91	399.55	432.73
	120	347.18	392.06	35.33	400.56	426.09
	192	351.51	393.64	36.82	388.71	426.06
31	Cured	397.49	405.2	31.45	392.74	415.17
	48	299.39	363.95	36.15	351.77	410.15
	120	394	411.44	52.99	378.35	421.63

	192	393.78	413.54	53.44	377.99	422.81

3.5 Conclusion

This chapter provided a detailed characterization of the high heat resistant CE/novolac type EP blends towards high temperature molding applications. The evaluation on the thermomechanical properties as well as the long-term high temperature storage degradation were discussed specifically focused on the effects of the resin composition, where the distinguished thermal degradation mechanisms on the low CE and the high CE polymers were addressed and demonstrated.

A screen test was done on different types of novolac type EP candidate to form copolymer with CE. All of the formulations exhibited much improved thermal resistance and T_g compared to the previously used biphenyl type EP in the CE/EP copolymer. Out of these resins, an ECN type EP showed the best performance in the long-term aging test and was selected for the formulation study. The CE/ECN blends were evaluated by various types of characterization methods and many properties showed a tradeoff characteristic regarding the CE/ECN molar ratio. A high triazine content was observed for the high CE content blends. The T_g was found to first increase and then kept constant at around 250 ºC when increasing the CE monomer feed ratio. The cease of continuous increase in T_g was explained by the decrease in crosslink density in these formulations due to the lack of multifunctional EP, despite the incorporation of rigid triazine structure. Similarly, the thermal decomposition behavior of the copolymers exhibited the competition between

triazine structure increase and crosslink density decrease when increasing CE feed ratio, where a higher T_i while lower T_p of these polymers was found. It can be concluded that the low CE content formulations were able to produce high T_g and high heat resistant resins.

The high temperature storage effects on the CE/ECN blends were investigated, where the low CE blends and the high CE blends have seen distinguished characteristics. Similar to the previously studied CE/ biphenyl EP system, the high CE ratio polymer experienced larger weight loss and severe warpage and blistering after aging at 250 ℃. The TMA test on the samples after aging revealed a first increase and then decrease T_g of the low CE polymers during aging, while the α_2 showed the opposite trend. This phenomenon indicated the further vitrification of the EP during initial aging, followed by the decomposition of network structure. On the other hand, the T_g of the high CE polymers monotonically decreased when exposed to high temperature and the α_2 change was hard to conclude. The chemical structure change in the aged samples were characterized by FTIR. In the low CE content formulations, the further curing during the initial aging was evidenced by the diminish of remaining epoxide signals and the formed ether bonds. Further aging of the samples followed the typical thermo-oxidation pattern seen in EP supported by the emerging hydroxyl and carbonyl groups. The high CE polymers were on the other hand mostly dominated by the hydrolysis degradations resulting in carbamate formation and decomposition. The thermal stability of the aged samples also showed large discrepancy depending on the CE content in the resin. Low CE polymers experienced the initial stage of decomposition during aging and the remaining part could still match well with the TGA profile of the unaged sample. However, the high CE resins showed a dramatically inferior heat resistance after short aging. With the conclusion from TMA and

FTIR, this instability was explained by the large thermal stress induced by the outgas from carbamate decomposition. The degradations in the high CE polymers are to be resolved based on their unique aging mechanism to utilize their potential for high temperature encapsulant application.

CHAPTER 4. SUMMARY AND SUGGESTED WORK

4.1 Summary

The industry has seen increasing interests in encapsulant materials serve in harsher environments. For example, the next generation of power semiconductors will be based on SiC technologies for high power applications, where the higher operation temperature (250 ºC) would be required for optimized performance. However, this temperature exceeds the stability limit of epoxy (EP) chemistry in the epoxy molding compound (EMC) used as encapsulant. To develop the resin capable of withstanding the heat while meet the requirement for molding application, the EP/triazine resin system was selected and characterized in this thesis based on cyanate ester (CE)/EP copolymerization chemistry. Two types of EP were evaluated in this thesis including the biphenyl type EP and the novolac type EP. In the CE/ biphenyl EP system, different approaches on chemical modifications have been proposed and demonstrated. In the CE/ novolac type EP system, the resin chemistry and thermomechanical properties were evaluated, with addressing the high temperature aging degradation mechanisms.

In Chapter 2, different approaches have been pursued to enhance the high temperature performance of the previously studied CE/ biphenyl EP blend where the inferior high temperature aging behavior in the high CE ratio blends was demonstrated despite their higher T_g and decomposition onset, which is mainly attributed to the hydrolysis degradation of remaining cyanate groups.

The effects of different metal catalyst on the CE properties were discussed, candidates include two types of active metal ions and two types of chelate ligands i.e. Al(III) acac, Cu(II) acac and Cu(II)bzac. The effects of active metal ion were found more dominant than the ligand structure. The Cu^{2+} ions were more efficient in facilitating while exhibiting lower tendency of forming carbamate in the Cu^{2+} catalysed CE resulted in a prolonged storage life under high temperature. In the CE/EP blends (1:1), two separate curing exotherms were evidenced in the Cu^{2+} catalysed polymers. These two peaks were identified to be trimerization of CE at low temperature and CE/EP copolymerization at high temperature.

A triazine containing molecule triglycidyl isocyanurate (TGIC) was employed as an epoxy source to increase the triazine content to increasing T_g and short-term heat resistant at low CE contents that can help reducing the presence of unreacted cyanate groups. The incorporation of TGIC increased the triazine and isocyanurate contents in the polymer, and the trifunctional nature of the molecule increased crosslink density. These features effectively increased the T_g of CE/EP blend at low loading. Further increasing the TGIC content can cause the plasticizing effects of unreacted small molecules and may reduce the T_g. The thermal decomposition behavior were also improved. However, due to the high moisture absorption rate in the TGIC incorporated polymers, a large weight loss during high temperature aging was observed.

The high heat resistant novolac type CE was employed to form the NCE/EP blend, and their blends with different feed ratio were systematically evaluated. The very high T_g over 400 ºC from DMA was observed in the pure NCE. The increase of NCE content in the NCE/EP blend significantly increased the T_g as well as decomposition onset of the

polymer. The EP on the other hand was found to dilute the viscos NCE and reduce the viscosity to render processability. The pure NCE exhibited superior heat resistance under 250 ºC aging condition than the NCE/EP blends in the first 700 hours while a large weight loss gradient and swelling was observed following that. The high moisture absorption plasticized the network and facilitated the hydrolysis degradation was the main cause of this behavior. All the blends showed a suppressed weight loss profile after the initial drop. The mid NCE content compositions have great potential for future high temperature molding applications with these intriguing features.

The Chapter 3 provided a detailed characterization of the high heat resistant CE/novolac type EP blends as well as the long-term high temperature storage degradation, where the distinguished thermal degradation mechanisms on the low CE and the high CE polymers were demonstrated.

A screen test was done on different types of novolac type EP candidate to form copolymer with CE. All of the formulations exhibited much improved thermal resistance and T_g compared to the previously used biphenyl type EP in the CE/EP copolymer. Out of these resins, an ECN type EP showed the best overall performance and was selected for the formulation study. In the CE/ECN blends, a high triazine content was observed for the high CE content polymers. The T_g and decomposition behaviors of these materials was found to exhibit a competition between increasing triazine content and decreasing crosslink density when increasing CE monomer feed. Low CE content formulations were able to produce high T_g and high heat resistant resins.

The high temperature storage effects on the CE/ECN blends were investigated, where the low CE blends and the high CE blends have seen distinguished characteristics. The high CE ratio polymer experienced larger weight loss and severe warpage and blistering after aging at 250 ºC. From the TMA, FTIR and TGA studies, it can be concluded that the dominating degradation mechanism was different for low CE and high CE polymers. The low CE content CE/ECN blends went through further curing in the initial aging, and the thermo-oxidation at the weak ether linkages became appreciable. The high CE polymers were suffered from the hydrolysis degradations from carbamate formation, resulted high stress in the resin that induced the instability. The degradations in the high CE polymers are to be resolved based on their unique aging mechanism to utilize their potential for high temperature encapsulant application.

4.2 Suggested Work

(1) To utilize the high temperature properties of CE while suppress the hydrolysis problems, it could be perused to reduce the moisture attack on cyanate groups through the substitution of methyl groups on ortho positions as a kinetic hindrance [83]. Its effects on affecting the CE/EP copolymerization and on the copolymer's properties could be investigated.

(2) The current chemistry requires substantial high temperature to cure, which not only slow down the production rate, but also can induce degradation of the resin in the curing cycle (for example the carbamate formation when exposed to moisture). The snap cure behavior of CE using encapsulated primary amine [84] could be interesting to incorporated in the CE/EP system and their performance on high temperature are to be studied.

(3) To be used in molding application, the large CTE mismatch between the resin and Si or substrate should be minimized through high filler loading. The property degradation pattern of the CE/EP mixed with inorganic fillers including their adhesions and mechanical properties should be evaluated. The demonstration of these molding material in the power module should be made and their reliability should be tested.

REFERENCES

[1] P. T. Krein, "1 - Introduction," in *Power Electronics Handbook (Third Edition)*, M. H. Rashid, Ed., ed Boston: Butterworth-Heinemann, 2011, pp. 1-14.

[2] Y. Liu, "Challenges of Power Electronic Packaging," in *Power Electronic Packaging: Design, Assembly Process, Reliability and Modeling*, Y. Liu, Ed., ed New York, NY: Springer New York, 2012, pp. 1-8.

[3] G. Zhang, Z. Li, B. Zhang, and W. A. Halang, "Power electronics converters: Past, present and future," *Renewable and Sustainable Energy Reviews,* vol. 81, pp. 2028-2044, 2018.

[4] Y. Yao, G.-Q. Lu, D. Boroyevich, and K. D. Ngo, "Survey of high-temperature polymeric encapsulants for power electronics packaging," *IEEE Transactions on Components, Packaging and Manufacturing Technology,* vol. 5, pp. 168-181, 2015.

[5] K. Shenai, R. S. Scott, and B. J. Baliga, "Optimum semiconductors for high-power electronics," *IEEE transactions on Electron Devices,* vol. 36, pp. 1811-1823, 1989.

[6] J. A. COOPERJR and A. Agarwal, "SiC power-switching devices—The second electronics revolution?," *Proceedings of the IEEE,* vol. 90, 2002.

[7] A. Bindra, "Wide-bandgap-based power devices: Reshaping the power electronics landscape," *IEEE Power Electronics Magazine,* vol. 2, pp. 42-47, 2015.

[8] C. Chen, F. Luo, and Y. Kang, "A review of SiC power module packaging: Layout, material system and integration," *CPSS Transactions on Power Electronics and Applications,* vol. 2, pp. 170-186, 2017.

[9] A. Mavinkurve, L. Goumans, and J. Martens, "Epoxy molding compounds for high temperature applications," in *2013 Eurpoean Microelectronics Packaging Conference (EMPC)*, 2013, pp. 1-7.

[10] D. Lu and C. Wong, *Materials for advanced packaging* vol. 181: Springer, 2009.

[11] N. Kinjo, M. Ogata, K. Nishi, A. Kaneda, and K. Dušek, "Epoxy molding compounds as encapsulation materials for microelectronic devices," in *Speciality Polymers/Polymer Physics*, ed: Springer, 1989, pp. 1-48.

[12] J. L. Hull, "Compression and transfer molding," *Handbook of Plastic Processes,* pp. 455-473, 2006.

[13] S. Rimdusit and H. Ishida, "Development of new class of electronic packaging materials based on ternary systems of benzoxazine, epoxy, and phenolic resins," *Polymer,* vol. 41, pp. 7941-7949, 2000.

[14] E. S. A. Rashid, K. Ariffin, C. C. Kooi, and H. M. Akil, "Preparation and properties of POSS/epoxy composites for electronic packaging applications," *Materials & Design,* vol. 30, pp. 1-8, 2009.

[15] P. Teh, M. Jaafar, H. Akil, K. Seetharamu, A. Wagiman, and K. Beh, "Thermal and mechanical properties of particulate fillers filled epoxy composites for electronic packaging application," *Polymers for Advanced Technologies,* vol. 19, pp. 308-315, 2008.

[16] L. Banks and B. Ellis, "The glass transition temperatures of highly crosslinked networks: Cured epoxy resins," *Polymer,* vol. 23, pp. 1466-1472, 1982.

[17] C. S. Wu, Y. L. Liu, Y. C. Chiu, and Y. S. Chiu, "Thermal stability of epoxy resins containing flame retardant components: an evaluation with thermogravimetric analysis," *Polymer degradation and stability,* vol. 78, pp. 41-48, 2002.

[18] L. H. Lee, "Mechanisms of thermal degradation of phenolic condensation polymers. II. Thermal stability and degradation schemes of epoxy resins," *Journal of Polymer Science Part A: General Papers,* vol. 3, pp. 859-882, 1965.

[19] F.-L. Jin and S.-J. Park, "Thermal properties of epoxy resin/filler hybrid composites," *Polymer degradation and stability,* vol. 97, pp. 2148-2153, 2012.

[20] R. Velmurugan and T. Mohan, "Room temperature processing of epoxy-clay nanocomposites," *Journal of materials science,* vol. 39, pp. 7333-7339, 2004.

[21] A. A. Kumar, M. Alagar, and R. Rao, "Synthesis and characterization of siliconized epoxy-1, 3-bis (maleimido) benzene intercrosslinked matrix materials," *Polymer,* vol. 43, pp. 693-702, 2002.

[22] G. Odegard and A. Bandyopadhyay, "Physical aging of epoxy polymers and their composites," *Journal of Polymer Science Part B: Polymer Physics,* vol. 49, pp. 1695-1716, 2011.

[23] Y. Yang, G. Xian, H. Li, and L. Sui, "Thermal aging of an anhydride-cured epoxy resin," *Polymer degradation and stability,* vol. 118, pp. 111-119, 2015.

[24] J. Pospíšil, Z. Horák, Z. Kruliš, S. Nešpůrek, and S.-i. Kuroda, "Degradation and aging of polymer blends I. Thermomechanical and thermal degradation," *Polymer Degradation and Stability,* vol. 65, pp. 405-414, 1999.

[25] D. Leveque, A. Schieffer, A. Mavel, and J.-F. Maire, "Analysis of how thermal aging affects the long-term mechanical behavior and strength of polymer–matrix composites," *Composites science and technology,* vol. 65, pp. 395-401, 2005.

[26] S. Noijen, R. Engelen, J. Martens, A. Opran, and O. van der Sluis, "On the epoxy moulding compound aging effect on package reliability," in *EuroSimE 2009-10th*

International Conference on Thermal, Mechanical and Multi-Physics Simulation and Experiments in Microelectronics and Microsystems, 2009, pp. 1-5.

[27] E. Nguegang, J. Franz, A. Kretschmann, and H. Sandmaier, "Aging effects of Epoxy Moulding Compound on the long-term stability of plastic package," in *2010 11th International Thermal, Mechanical & Multi-Physics Simulation, and Experiments in Microelectronics and Microsystems (EuroSimE)*, 2010, pp. 1-6.

[28] Y.-m. Pei, K. Wang, M.-s. Zhan, W. Xu, and X.-j. Ding, "Thermal-oxidative aging of DGEBA/EPN/LMPA epoxy system: Chemical structure and thermal–mechanical properties," *Polymer degradation and Stability,* vol. 96, pp. 1179-1186, 2011.

[29] J. De Vreugd, A. S. Monforte, K. Jansen, L. Ernst, C. Bohm, A. Kessler, *et al.*, "Effect of postcure and thermal aging on molding compound properties," in *2009 11th Electronics Packaging Technology Conference*, 2009, pp. 342-347.

[30] T. Ellis and F. Karasz, "Interaction of epoxy resins with water: the depression of glass transition temperature," *Polymer,* vol. 25, pp. 664-669, 1984.

[31] G. Xiao, M. a. Delamar, and M. Shanahan, "Irreversible interactions between water and DGEBA/DDA epoxy resin during hygrothermal aging," *Journal of Applied Polymer Science,* vol. 65, pp. 449-458, 1997.

[32] F.-L. Jin, X. Li, and S.-J. Park, "Synthesis and application of epoxy resins: A review," *Journal of Industrial and Engineering Chemistry,* vol. 29, pp. 1-11, 2015.

[33] M. Ogata, N. Kinjo, and T. Kawata, "Effects of crosslinking on physical properties of phenol–formaldehyde novolac cured epoxy resins," *Journal of applied polymer science,* vol. 48, pp. 583-601, 1993.

[34] Y. Tanaka and I. Watanabe, "Latest developments of molding compound material for power semiconductors," in *2018 China Semiconductor Technology International Conference (CSTIC)*, 2018, pp. 1-3.

[35] C. B. Bucknall and A. H. Gilbert, "Toughening tetrafunctional epoxy resins using polyetherimide," *Polymer,* vol. 30, pp. 213-217, 1989.

[36] A. Bonnet, B. Lestriez, J. Pascault, and H. Sautereau, "Intractable high ‐ Tg thermoplastics processed with epoxy resin: Interfacial adhesion and mechanical properties of the cured blends," *Journal of Polymer Science Part B: Polymer Physics,* vol. 39, pp. 363-373, 2001.

[37] K. Mimura, H. Ito, and H. Fujioka, "Improvement of thermal and mechanical properties by control of morphologies in PES-modified epoxy resins," *Polymer,* vol. 41, pp. 4451-4459, 2000.

[38] B. Francis, S. Thomas, J. Jose, R. Ramaswamy, and V. L. Rao, "Hydroxyl terminated poly (ether ether ketone) with pendent methyl group toughened epoxy resin: miscibility, morphology and mechanical properties," *Polymer,* vol. 46, pp. 12372-12385, 2005.

[39] A. K. S. Clair and T. L. S. Clair, "High temperature polyimide film laminates and process for preparation thereof," ed: Google Patents, 1985.

[40] R. J. Iredale, C. Ward, and I. Hamerton, "Modern advances in bismaleimide resin technology: a 21st century perspective on the chemistry of addition polyimides," *Progress in Polymer Science,* vol. 69, pp. 1-21, 2017.

[41] C. P. R. Nair, D. Mathew, and K. N. Ninan, "Cyanate Ester Resins, Recent Developments," in *New Polymerization Techniques and Synthetic Methodologies*, ed Berlin, Heidelberg: Springer Berlin Heidelberg, 2001, pp. 1-99.

[42] I. Hamerton and J. N. Hay, "Recent developments in the chemistry of cyanate esters †," *Polymer International,* vol. 47, pp. 465-473, 1998.

[43] T. M. Keller, "Phthalonitrile-based high temperature resin," *Journal of Polymer Science Part A: Polymer Chemistry,* vol. 26, pp. 3199-3212, 1988.

[44] L.-S. Tan and F. E. Arnold, "Benzocyclobutene in polymer synthesis. I. Homopolymerization of bisbenzocyclobutene aromatic imides to form high-temperature resistant thermosetting resins," *Journal of Polymer Science Part A: Polymer Chemistry,* vol. 26, pp. 1819-1834, 1988.

[45] F.-L. Jin and S.-J. Park, "Thermal properties and toughness performance of hyperbranched-polyimide-modified epoxy resins," *Journal of Polymer Science Part B: Polymer Physics,* vol. 44, pp. 3348-3356, 2006.

[46] J. Seo, W. Jang, and H. Han, "Thermal properties and water sorption behaviors of epoxy and bismaleimide composites," *Macromolecular Research,* vol. 15, pp. 10-16, February 01 2007.

[47] T.-H. Ho, H.-J. Hwang, J.-Y. Shieh, and M.-C. Chung, "Thermal, physical and flame-retardant properties of phosphorus-containing epoxy cured with cyanate ester," *Reactive and Functional Polymers,* vol. 69, pp. 176-182, 2009/03/01/ 2009.

[48] I. Hamerton, "High-Performance Thermoset–Thermoset Polymer Blends: A Review of the Chemistry of Cyanate Ester–Bismaleimide Blends," *High Performance Polymers,* vol. 8, pp. 83-95, 1996/03/01 1996.

[49] R. P. Singh, M. Zhang, and D. Chan, "Toughening of a brittle thermosetting polymer: Effects of reinforcement particle size and volume fraction," *Journal of Materials Science,* vol. 37, pp. 781-788, 2002/02/01 2002.

[50] S. Robitaille, "Cyanate Ester Resins," in *Composites* vol. 21, D. B. Miracle and S. L. Donaldson, Eds., ed: ASM International, 2001, p. 0.

[51] I. Hamerton and J. N. Hay, "Recent Technological Developments in Cyanate Ester Resins," *High Performance Polymers,* vol. 10, pp. 163-174, 1998/06/01 1998.

[52] T. Fang and D. A. Shimp, "Polycyanate esters: Science and applications," *Progress in Polymer Science,* vol. 20, pp. 61-118, 1995/01/01/ 1995.

[53] V. Viner, "Frontal polymerization of a cyanate ester," *Journal of Applied Polymer Science,* vol. 128, pp. 2208-2215, 2013/05/05 2013.

[54] M. R. Kessler, "Cyanate Ester Resins Adapted from Cyanate Ester Resins, First Edition," *Wiley Encyclopedia of Composites,* pp. 1-15, 2012/07/20 2012.

[55] A. Osei-Owusu, G. C. Martin, and J. T. Gotro, "Catalysis and kinetics of cyclotrimerization of cyanate ester resin systems," *Polymer Engineering & Science,* vol. 32, pp. 535-541, 1992/04/01 1992.

[56] D. A. Shimp, "Metal acetylacetonate/alkylphenol curing catalyst for polycyanate esters of polyhydric phenols," ed: Google Patents, 1989.

[57] D. A. Shimp, "Metal acetylacetonate/alkylphenol curing catalyst for polycyanate esters of polyhydric phenols," ed: Google Patents, 1988.

[58] M. Gaku, K. Suzuki, and K. Nakamichi, "Curable resin compositions of cyanate esters," ed: Google Patents, 1978.

[59] B. S. Kim, "Effect of cyanate ester on the cure behavior and thermal stability of epoxy resin," *Journal of applied polymer science,* vol. 65, pp. 85-90, 1997.

[60] R. H. Lin, "In situ FTIR and DSC investigation on cure reaction of liquid aromatic dicyanate ester with different types of epoxy resin," *Journal of Polymer Science Part A: Polymer Chemistry,* vol. 38, pp. 2934-2944, 2000.

[61] W. F. Su and C. M. Chuang, "Effects of chemical structure changes on curing reactions and thermal properties of cyanate ester ‐ cured rigid ‐ rod epoxy resins," *Journal of applied polymer science,* vol. 85, pp. 2419-2422, 2002.

[62] P. Ren, G. Liang, and Z. Zhang, "Epoxy ‐ modified cyanate ester resin and its high ‐ modulus carbon ‐ fiber composites," *Polymer composites,* vol. 27, pp. 402-409, 2006.

[63] Y. Lei, M. Xu, M. Jiang, Y. Huang, and X. Liu, "Curing behaviors of cyanate ester/epoxy copolymers and their dielectric properties," *High Performance Polymers,* vol. 29, pp. 1175-1184, 2017.

[64] Z. Ren, Y. Cheng, L. Kong, and F. Xiao, "Preparation and characterization of a high Tg cyanate ester/epoxy composite resin," in *2014 15th International Conference on Electronic Packaging Technology*, 2014, pp. 288-291.

[65] C. Sakthidharan, P. Sundararajan, and M. Sarojadevi, "Thermal and mechanical properties of azomethine functionalized cyanate ester/epoxy blends," *RSC Advances,* vol. 5, pp. 19666-19674, 2015.

[66] L. Jayakumari, V. Thulasiraman, and M. Sarojadevi, "Synthesis and characterization of cyanate epoxy composites," *High Performance Polymers,* vol. 19, pp. 33-47, 2007.

[67] D. Mathew, R. Nair, and K. Ninan, *Bisphenol A dicyanate–novolac epoxy blend: Cure characteristics, physical and mechanical properties, and application in composites* vol. 74, 1999.

[68] B. Guo, W. Fu, D. Jia, Q. Qiu, and L. Wang, "Cure behaviour and structure of dicyanate-epoxy novolac blends," *Polymers and Polymer Composites,* vol. 10, pp. 237-248, 2002.

[69] F. Wu, C.-C. Tuan, B. Song, K.-S. Moon, and C.-P. Wong, "Controlled synthesis and evaluation of cyanate ester/epoxy copolymer system for high temperature molding compounds," *Journal of Polymer Science Part A: Polymer Chemistry,* vol. 56, pp. 1337-1345, 2018.

[70] D. Mathew, C. P. Reghunadhan Nair, and K. N. Ninan, "Bisphenol A dicyanate–novolac epoxy blend: Cure characteristics, physical and mechanical properties, and application in composites," *Journal of Applied Polymer Science,* vol. 74, pp. 1675-1685, 1999.

[71] J. D. Sudha, S. Pradhan, H. Viswanath, J. Unnikrishnan, P. Brahmbhatt, and M. S. Manju, "Studies on the cure parameters of cyanate ester–epoxy blend system through rheological property measurements," *Journal of Thermal Analysis and Calorimetry,* vol. 115, pp. 743-750, January 01 2014.

[72] Q. Song, Y. Ding, Z. L. Wang, and Z. J. Zhang, "Tuning the thermal stability of molecular precursors for the nonhydrolytic synthesis of magnetic MnFe2O4 spinel nanocrystals," *Chemistry of Materials,* vol. 19, pp. 4633-4638, 2007.

[73] S. Pinchas and D. Ben-Ishai, "The Carbonyl Absorption of Carbamates and 2-Oxazolidones in the Infrared Region," *Journal of the American Chemical Society,* vol. 79, pp. 4099-4104, 1957/08/01 1957.

[74] D. Parra, L. P. Mercuri, J. d. R. Matos, H. F. d. Brito, and R. Romano, "Thermal behavior of the epoxy and polyester powder coatings using thermogravimetry/differential thermal analysis coupled gas chromatography/mass spectrometry (TG/DTA–GC/MS) technique: identification of the degradation products," *Thermochimica Acta,* vol. 386, pp. 143-151, 2002.

[75] H. Khonakdar, J. Morshedian, U. Wagenknecht, and S. Jafari, "An investigation of chemical crosslinking effect on properties of high-density polyethylene," *Polymer,* vol. 44, pp. 4301-4309, 2003.

[76] N. Rose, M. Le Bras, S. Bourbigot, and R. Delobel, "Thermal oxidative degradation of epoxy resins: evaluation of their heat resistance using invariant kinetic parameters," *Polymer degradation and stability,* vol. 45, pp. 387-397, 1994.

[77] S. K. Karad, D. Attwood, and F. R. Jones, "Moisture absorption by cyanate ester modified epoxy resin matrices. Part III. Effect of blend composition," *Composites Part A: Applied Science and Manufacturing,* vol. 33, pp. 1665-1675, 2002.

[78] K. Unnikrishnan and E. Thachil, "Aging and thermal studies on epoxy resin modified by epoxidized novolacs," *Polymer-Plastics Technology and Engineering,* vol. 45, pp. 469-474, 2006.

[79] S. Levchik, A. Piotrowski, E. Weil, and Q. Yao, "New developments in flame retardancy of epoxy resins," *Polymer Degradation and Stability,* vol. 88, pp. 57-62, 2005.

[80] C. Bockenheimer, D. Fata, and W. Possart, "New aspects of aging in epoxy networks. I. Thermal aging," *Journal of Applied Polymer Science,* vol. 91, pp. 361-368, 2004.

[81] L. J. Kasehagen, I. Haury, C. W. Macosko, and D. A. Shimp, "Hydrolysis and blistering of cyanate ester networks," *Journal of Applied Polymer Science,* vol. 64, pp. 107-113, 1997.

[82] S. V. Levchik and E. D. Weil, "Thermal decomposition, combustion and flame-retardancy of epoxy resins—a review of the recent literature," *Polymer International,* vol. 53, pp. 1901-1929, 2004.

[83] A. J. Guenthner, M. E. Wright, A. P. Chafin, J. T. Reams, K. R. Lamison, M. D. Ford*, et al.*, "Mechanisms of decreased moisture uptake in ortho-methylated di (cyanate ester) networks," *Macromolecules,* vol. 47, pp. 7691-7700, 2014.

[84] J. Bauer and M. Bauer, "Cyanate ester based resin systems for snap-cure applications," *Microsystem technologies,* vol. 8, pp. 58-62, 2002.

PUBLICATIONS OF THE AUTHOR

[1] **J.Li**, B. Song, K. Moon, J. Hah, X. Wang, R. Zhang, *et al.*, " High temperature treatment for preparing polysulfide sealant/Ag composite with high electrical conductivity and its mechanism," *Composites Part B: Engineering*, submitted.

[2] **J.Li**, C. Ren, K. Moon and C.P. Wong, " Epoxy/ triazine copolymer resin system for high temperature encapsulant applications," in *2019 69th Electronic Components and Technology Conference,* in press, 2019.

[3] **J.Li**, C. Ren, K. Moon and C.P. Wong, " Evaluation and aging degradation onc yanate ester/epoxy cresol novolac copolymer system for high temperature encapsulant applications,", in preparation.

[4] B. Song, **J. Li**, F. Wu, S. Patel, J. Hah, X. Wang*, et al.*, "Processing and characterization of silver-filled conductive polysulfide sealants for aerospace applications," *Soft matter,* vol. 14, pp. 9036-9043, 2018.